

**Key Words:**  
**Distribution Coefficient**  
**Cement**  
**Saltstone**  
**Performance Assessment**  
**Vault**

**Retention:**  
**Permanent**

## **VARIABILITY OF $K_d$ VALUES IN CEMENTITIOUS MATERIALS AND SEDIMENTS**

**P. M. Almond**  
**D. I. Kaplan**  
**E. P. Shine**

**JANUARY 2012**

Savannah River National Laboratory  
Savannah River Nuclear Solutions  
Aiken, SC 29808

**Prepared for the U.S. Department of Energy Under  
Contract Number DE-AC09-08SR22470**



**DISCLAIMER**

**This work was prepared under an agreement with and funded by the U.S. Government. Neither the U. S. Government or its employees, nor any of its contractors, subcontractors or their employees, makes any express or implied:**

- 1. warranty or assumes any legal liability for the accuracy, completeness, or for the use or results of such use of any information, product, or process disclosed; or**
- 2. representation that such use or results of such use would not infringe privately owned rights; or**
- 3. endorsement or recommendation of any specifically identified commercial product, process, or service.**

**Any views and opinions of authors expressed in this work do not necessarily state or reflect those of the United States Government, or its contractors, or subcontractors.**

**Printed in the United States of America**

**Prepared for  
U.S. Department of Energy**

**Key Words:**  
**Distribution Coefficient**  
**Cement**  
**Saltstone**  
**Performance Assessment**  
**Vault**

**Retention:**  
**Permanent**

## **VARIABILITY OF $K_d$ VALUES IN CEMENTITIOUS MATERIALS AND SEDIMENTS**

**P. M. Almond**  
**D. I. Kaplan**  
**E. P. Shine**

**JANUARY 2012**

Savannah River National Laboratory  
Savannah River Nuclear Solutions  
Savannah River Site  
Aiken, SC 29808

---

**Prepared for the U.S. Department of Energy Under  
Contract Number DE-AC09-08SR22470**



# TABLE OF CONTENTS

LIST OF FIGURES .....	iv
LIST OF TABLES .....	v
LIST OF ACRONYMS .....	vi
1.0 EXECUTIVE SUMMARY .....	7
2.0 INTRODUCTION.....	9
3.0 EXPERIMENTAL.....	10
3.1 Sample Selection and Characterization - Cementitious Samples .....	10
3.2 Materials and Methods .....	13
3.2.1 Materials - Cementitious Materials .....	14
3.2.2 Methods - Cementitious Materials.....	14
3.2.3 Materials and Methods - Soil Samples .....	15
3.2.4 Statistical Approach – Distribution Model Comparisons .....	15
4.0 RESULTS AND DISCUSSION .....	16
4.1 Cesium Measured in Cementitious Materials.....	18
4.1.1 Cesium $K_d$ Model Comparisons of Distribution Fits: .....	20
4.2 Strontium $K_d$ Values Measured in Cementitious Materials .....	22
4.2.1 Strontium $K_d$ Model Comparisons of Distribution Fits.....	23
4.3 Iodine Measured in Cementitious Materials.....	26
4.3.1 Iodine $K_d$ Model Comparisons of Distribution Fits .....	27
4.4 Europium Measured in Cementitious Materials.....	30
4.5 Effect of Cement cure Temperature on Distribution coefficients in Cementitious Materials.....	30
4.6 Plutonium Distribution Coefficients Measured in Soils.....	30
4.6.1 Entire Pu $K_d$ Data Set: All pH Values.....	35
4.6.2 pH >7.0 Pu $K_d$ Data Set .....	39
4.6.3 Pu $K_d$ Data Set for pH $\leq$ 7.0 .....	41
4.6.4 Subsets of the Pu $K_d$ Data Set based on pH and Sediment Texture .....	44
4.6.5 Input Weibull Distribution Values .....	45
4.6.6 Recommended Values for Performance Assessments.....	45
5.0 CONCLUSIONS .....	47
6.0 REFERENCES.....	49
7.0 APPENDIX A: SUPPORTING STATISTICAL ANALYSES .....	52
7.1 Saltstone $K_d$ Values .....	53
7.2 Soil PLutonium $K_d$ Values .....	60
8.0 APPENDIX B: Pu(IV) and Pu(V) Sorption Edge at 24 Hr or 33 Days (Powell et al. 2002) .....	66

## LIST OF FIGURES

Figure 1. (TOP) The Frechet distribution of the Cs $K_d$ Saltstone data set. Plot on left (quantile) is a linear version of plot on right (nonparametric). Shaded region provides 95% confidence region. Note no points outside shaded zone. Frechet distribution fits the low- and mid $K_d$ values especially well. (MIDDLE) The Loglogistic distribution of the Cs $K_d$ saltstone data set quantile (left) and nonparametric (right). Note that there are three or four data points outside the shaded region and the low $K_d$ fit is poor even though the general goodness-of-fit is very acceptable. (BOTTOM) Lognormal distribution of Cs $K_d$ saltstone data set quantile (left and nonparametric (right) Of the three models, this one is the poorest. ....	21
Figure 2. Lognormal, loglogistic and Frechet quantile and nonparametric plots of the Sr $K_d$ Saltstone data. Shaded region provides 95% confidence region. Compared to the Frechet, the loglogistic distribution seems to be a bit better than the Frechet for low $K_d$ values, and near the “elbow” of the graph. ....	25
Figure 3. Zero-inflated distribution models to the iodine saltstone $K_d$ values: Lognormal, Weibull, Loglogistic, and Frechet. The "Zero-inflated" indicates that the negative $K_d$ values were assigned zero values and treated uniquely in the distribution model. ....	29
Figure 4. Lognormal and Weibull distribution fits to the entire data set of sediment Pu $K_d$ values. The red dots indicate $pH > 7.0$ and blue dots indicate $pH \leq 7$ . Shaded area is the 95% confidence region. ....	38
Figure 5. Weibull fits to the quantile plot (left) and nonparametric plot (right). ....	40
Figure 6. Weibull, lognormal Exponential and Extended Generalized Gamma model fits to the Pu $K_d$ data of $pH \leq 7$ . ....	43
Figure 7. Histogram of Cs $\log K_d$ distribution data of 2-component normal fit demonstrating the potential presence of a second high temperature population. ....	54
Figure 8 Weibull, Loglogistic, and Lognormal fits to the sand data for $pH \leq 7$ . The left graphs plot the cumulative probability vs. $K_d$ on a linear scale, and the graphs on the right plot $K_d$ on a scale that should result in a straight line if the intended distribution is correct. .	61
Figure 9. Pu(IV) and Pu(V) sorption edge at 24 hr or 33 days on: (A) subsurface sandy sediment, (B) subsurface clayey sediment, (C) surface sandy sediment, and (D) surface clayey sediment (Powell et al. 2002). ....	67

## LIST OF TABLES

Table 1. Samples selected for $K_d$ variability study and key variables. ....	11
Table 2. Simulant components and concentrations (Molarity) for selected samples. ....	12
Table 3. Sample heating profiles. ....	12
Table 4 . $K_d$ values (mL/g) calculated from adsorption experiments for cesium, strontium, and iodine. ....	17
Table 5. Previously reported $K_d$ values for cementitious materials under oxidizing and reducing conditions. ....	17
Table 6. Plots and descriptive statistics for Cs $K_d$ values in saltstone. ....	19
Table 7. Goodness-of-fit of distribution models for Cs $K_d$ values in saltstone. ....	20
Table 8. Plots and descriptive statistics for Sr $K_d$ values in saltstone. ....	23
Table 9. Goodness-of-fit of distribution models for Sr $K_d$ values in saltstone. ....	24
Table 10. Plot and descriptive statics for iodine $K_d$ values in saltstone. ....	27
Table 11. Goodness-of-fit of distribution models for iodine $K_d$ values in saltstone. ....	28
Table 12. Pu $K_d$ values selected from the literature used to develop the Pu $K_d$ sediment distribution (sorted by pH). ....	32
Table 13. Characterization of sediments used in Pu $K_d$ measurements discussed in Table 12. ....	34
Table 14. Quantiles and descriptive statistics of the full data set of Pu $K_d$ values. ....	36
Table 15. Goodness-of-fit of distribution models for full data set of $K_d$ values in soil. ....	36
Table 16. Quantiles and descriptive statistics of the pH >7.0 Pu $K_d$ data set. ....	39
Table 17. Goodness-of-fit of distribution models for the pH >7.0 Pu $K_d$ data set. ....	40
Table 18. Quantiles and descriptive statistics of the pH $\leq$ 7.0 Pu $K_d$ data set. ....	41
Table 19. Goodness-of-fit of distribution models for the Pu $K_d$ data set for $\leq$ pH 7.0. ....	42
Table 20. Quantile and statistical analysis of sediment Pu $K_d$ values in entire data set, sandy sediment, and clayey sediments. ....	44
Table 21. Parametric Estimate for GoldSim Calculated from Statistical Modeling of Weibull Distributions for Pu $K_d$ Values. ....	45
Table 22. Input GoldSim Parametric Estimates for the Zero-Inflated Weibull Distributions for Cement Iodine $K_d$ Values. ....	45
Table 23. Recommended Parametric Estimate for Weibull Distributions for Pu $K_d$ Values . ....	46
Table 24. Saltstone Cs, Sr, and iodine $K_d$ average and standard deviation. ....	53
Table 25. Correlation coefficients for cesium, strontium and iodine saltstone $K_d$ values and saltstone properties. ....	54
Table 26. Cs $K_d$ values (mL/g) as a function of temperature curing ranges. ....	55
Table 27. Statistics for relative goodness of fit model comparisons for sand with pH $\leq$ 7. ....	60
Table 28. Quantile and characterization statistics of the Sand or Clay Pu $K_d$ values for varying pH ranges. ....	62

## LIST OF ACRONYMS

AD	Analytical Development
AIC	Akaike Information Criterion
AICc	Akaike Information Criterion with correction
BIC	Schwartz's Bayesian information criterion
ARP	Actinide Removal Process
BFS	Blast Furnace Slag
C-H-S	Calcium Silicate Hydrogel (variable C – S ratio)
Ca(OH) <sub>2</sub>	Portlandite
CSSX	Caustic Side Solvent Extraction
CV	Coefficient of Variation
DI	Deionized
DDA	Deliquification, Dissolution, and Adjustment
DSS	Decontaminated Salt Solution
FA	Fly Ash
K <sub>d</sub>	Distribution coefficient
MCU	Modular CSSX Unit
PA	Performance Assessment
OPC	Ordinary Portland Cement
ORP	Oxidation-Reduction Potential
SDF	Saltstone Disposal Facility
SPF	Saltstone Production Facility
SHE	Standard Hydrogen Electrode
SRNL	Savannah River National Laboratory
SRNS	Savannah River Nuclear Solutions
SRS	Savannah River Site
SWPF	Salt Waste Processing Facility

## 1.0 EXECUTIVE SUMMARY

Measured distribution coefficients ( $K_d$  values) for environmental contaminants provide input data for performance assessments (PA) on the Savannah River Site (SRS) that evaluate physical and chemical phenomena for release of radionuclides from wasteforms, degradation of engineered components and subsequent transport of radionuclides through environmental media. This report contains results from two tasks. The first task measured Cs, Sr, I, and Eu  $K_d$  values with simulated saltstone. The second task consisted of a critical literature review and statistical analysis of soil Pu  $K_d$  values. For both tasks the statistical range and distribution were determined to assist stochastic modelers in site wide PA analyses.

*Saltstone  $K_d$  Task* – The objective of the saltstone  $K_d$  variability project was to determine the range and distribution of cesium, strontium, iodine and europium  $K_d$  values in saltstone. The scope of this study did not include understanding saltstone sorption mechanisms responsible for increasing or decreasing sorption. Cs, Sr, and I  $K_d$  values were measured from a wide range of formulations of 22 archived saltstone materials (measured in triplicate). Eu  $K_d$  values could not be measured because Eu precipitated or sorbed to glassware during the experiment. The following  $K_d$  ranges, means, and standard deviations were obtained:

- saltstone triplicate Cs  $K_d$  values ranged from 5 to 436 mL/g (mean  $K_d = 20 \pm 15$  mL/g for <60 °C samples; mean  $K_d = 289 \pm 115$  mL/g for 60 °C samples),
- saltstone triplicate Sr  $K_d$  values ranged from 122 to 6,938 mL/g (mean  $K_d = 528 \pm 242$  mL/g for <60 °C samples; mean  $K_d = 3383 \pm 2401$  mL/g for 60 °C samples)
- saltstone triplicate I  $K_d$  values ranged from -1.5 to 2.9 mL/g (mean  $K_d = 1.07 \pm 0.97$  mL/g for all samples)

The distribution of saltstone  $K_d$  values were very wide, capturing the wide array of formulations and temperature curing conditions represented in the samples.

This work suggests keeping the present method of calculating  $K_d$  value ranges for stochastic models:

$$\begin{aligned}\text{“Min”} &= K_d - (1.5 * 0.5 * K_d) = 0.25 * K_d \\ \text{“Max”} &= K_d + (1.5 * 0.5 * K_d) = 1.75 * K_d\end{aligned}$$

This range is not as large as identified experimentally. It is possible that the experimental conditions selected are not in fact those that may prevail in the field. Furthermore, only a small number of samples were analyzed. Two types of distributions were selected for the cementitious materials. Lognormal is used for the cations (Cs, Sr etc...) and the zero-inflated Weibull for the anions that used  $K_d$  values including  $K_d = 0$  (e.g. I). The Weibull and lognormal are very common distributions that are available in the GoldSim software presently used on the SRS for stochastic modeling for various PAs.



*Soil Pu K<sub>d</sub> Task* – The range and distribution of plutonium K<sub>d</sub> values in soils is not known. 65 SRS sediment Pu-K<sub>d</sub> values were critically reviewed, tabulated, and then statistically analyzed to identify their range and distributions, similar to what was done with the saltstone K<sub>d</sub> values. Further refinement of the distributions was made based on the soil texture and soil pH range. The purpose of the Pu sediment K<sub>d</sub> dataset was not to attempt to understand through statistics how to better understand Pu sorption to sediments or to lower Pu K<sub>d</sub> variance. The following K<sub>d</sub> ranges, means, and standard deviations were obtained:

- pH 4.6 to 10.47 sediment Pu K<sub>d</sub> values ranged from 100 to 50,000 mL/g (mean K<sub>d</sub> =  $8,559 \pm 10,823$  mL/g; to simulate a plume moving through all pH conditions),
- pH 4.6 to 7.0 sediment Pu K<sub>d</sub> values ranged from 100-33,000 mL/g (mean =  $6,047 \pm 6,971$  mL/g ; to simulate a plume moving through far-field conditions),
- pH 7.01 to 10.47 sediment Pu K<sub>d</sub> values ranged from 210 – 50,000 mL/g (mean =  $12,851 \pm 14,525$  mL/g; to simulate a plume moving through a basic cementitious plume conditions), and

The Weibull distribution was recommended for each of the Pu sediment distributions. The large range in Pu K<sub>d</sub> was a result of a sharp rise or drop in K<sub>d</sub> values, consequently, if the intent is to reduce the range of K<sub>d</sub> values, then smaller ranges of pH values are recommended. The recommended best estimate Pu K<sub>d</sub> value for sandy sediments was increased from 290 to 650 mL/g based on long-term field lysimeter studies, and the observation that the 290 mL/g value was within the 10-25 percentile of Pu K<sub>d</sub> values in sandy sediments.

## 2.0 INTRODUCTION

Measured distribution coefficients ( $K_d$  values) for environmental contaminants provide input data for performance assessments (PA) that evaluate physical and chemical phenomena for release of radionuclides from wasteforms, degradation of engineered components and subsequent transport of radionuclides through environmental media. Research efforts at SRNL to study the effects of formulation and curing variability on the physiochemical properties of the saltstone wasteform produced at the Saltstone Disposal Facility (SDF) are ongoing and provide information for the PA and Saltstone Operations. Furthermore, the range and distribution of plutonium  $K_d$  values in soils is not known. Knowledge of these parameters is needed to provide guidance for stochastic modeling in the PA.

Under the current SRS liquid waste processing system, supernate from F & H Tank Farm tanks is processed to remove actinides and fission products, resulting in a low-curie Decontaminated Salt Solution (DSS). At the Saltstone Production Facility (SPF), DSS is mixed with premix, comprised of blast furnace slag (BFS), Class F fly ash (FA), and portland cement (OPC) to form a grout mixture. The fresh grout is subsequently placed in SDF vaults where it cures through hydration reactions to produce saltstone, a hardened monolithic waste form.

Variation in saltstone composition and cure conditions of grout can affect the saltstone's physiochemical properties. Variations in properties may originate from variables in DSS, premix, and water to premix ratio, grout mixing, placing, and curing conditions including time and temperature (Harbour et al. 2007; Harbour et al. 2009).

There are no previous studies reported in the literature regarding the range and distribution of  $K_d$  values in cementitious materials. Presently, the Savannah River Site (SRS) estimate ranges and distributions of  $K_d$  values based on measurements of  $K_d$  values made in sandy SRS sediments (Kaplan 2010). The actual cementitious material  $K_d$  values and solubility values differ from the sandy sediments. The  $K_d$  value range and distribution currently used in the PA are estimated to range between  $0.25 \cdot K_d$  and  $1.75 \cdot K_d$ , where the minimum and maximum values of the ranges reflect the 95% confidence level for the mean  $K_d$  value (Kaplan 2010).

The objective of the research with cementitious materials was to measure the range and distribution of a monovalent (Cs) and  $I^-$  (anion), divalent (Sr), and trivalent (Eu) ions for a variety of laboratory-prepared saltstone surrogate samples to establish a  $K_d$  range other than that which is presently used in the PA. It has been observed in laboratory samples that cure temperature profiles can affect properties such as heat of hydration, permeability, porosity, compressive strength, and set time (Harbour et al. 2009). The intent was to identify a range and distribution that could be used by stochastic modelers for the PA. Furthermore, the intent was to replace the arbitrarily selected distributions based on geological sandy sediments and to base it on actual cementitious materials. The scope of this study did not include understanding saltstone sorption mechanisms responsible for increasing or decreasing sorption.

Similar to the work with cementitious materials, the purpose of the Pu sediment  $K_d$  dataset was not to attempt to understand through statistics how to better understand Pu sorption to sediments

or to lower Pu  $K_d$  variance. The sediment Pu  $K_d$  data is included in this study because it is a key risk driver for the PAs on the SRS, and there is presently no direct studies of Pu variability in SRS soils. Instead the distribution of Pu sediment  $K_d$  values was assumed to be similar to other cations, as presented by Kaplan (2010).

### **3.0 EXPERIMENTAL**

#### **3.1 SAMPLE SELECTION AND CHARACTERIZATION - CEMENTITIOUS SAMPLES**

Twenty-two unique cementitious samples were selected from hundreds of archived samples that were prepared between 2008 to 2011 as part of Saltstone Variability studies and have relevance to saltstone performance (Table 1). Archived samples were initially inventoried to identify availability of the samples. Information from all located samples was compiled and was subsequently down selected to twenty-two to be used for experiment. The samples contained variation in their composition and preparation conditions, and these variables included, initial cure temperature profile, premix ratio, water to premix ratio, simulant solution, aluminate concentration, and sample age (Table 1, Table 3). The samples had been archived in labeled plastic bags or a capped plastic molds. Sample information was available in SRNL laboratory notebooks (Grout Variability Study 1-7) and SRNL reports (Harbour 2008, 2009).

Table 1. Samples selected for  $K_d$  variability study and key variables.

Sample Identification <sup>1</sup>	Simulant <sup>2</sup>	Premix Ratio (FA/Slag/OPC)	Water to Premix Ratio	Aluminate Concentration	Max Controlled Cure Temp (°C) <sup>3</sup>	Sample Age (Years)
GVS-88	SWPF	45/45/10	0.60	0.11	60	2.9
GVS-93	SWPF	30/60/10 <sup>3</sup>	0.60	0.45	22	2.9
GVS-94	SWPF	45/45/10	0.60	0.45	22	2.9
GVS-100-01	SWPF	45/45/10	0.60	0.28	22	2.8
GVS-100-02	SWPF	45/45/10	0.60	0.28	60	2.8
GVS-107	MCU	45/45/10	0.60	0.05	22	2.6
GVS-110	MCU	45/45/10	0.59	0.22	22	2.6
GVS-111	MCU	45/45/10	0.64	0.22	22	2.6
GVS-114	MCU	30/60/10	0.59	0.22	22	2.6
GVS-118	MCU	25/45/30	0.60	0.22	22	2.5
GVS-121	SWPF	45/45/10	0.60	0.35	22	2.2
GVS-123	SWPF	45/45/10	0.60	0.55	22	2.2
TR-419	MCU	45/45/10	0.60	0.05	22	3.7
TR-503	MCU	45/45/10	0.50	0.05	22	3.1
TR-513	SWPF	45/45/10	0.45	0.11	22	3.0
TR-517	MCU	45/45/10	0.60	0.05	40	3.0
TR-531	DDA	45/45/10	0.60	0.07	22	3.0
TR-614	MCU	25/45/30	0.60	0.22	22	2.2
TR-616	MCU	45/45/10	0.55	0.22	40	2.2
TP-006-003	Tank 50	45/45/10	0.55	0.28	41	0.8
TP-006-004	Tank 50	45/45/10	0.55	0.28	48	0.8
TP-006-005	Tank 50	45/45/10	0.55	0.28	57	0.8

<sup>1</sup>Similar samples are grouped together by white or gray shading.<sup>2</sup>See Table 2 for simulant composition for each sample.<sup>3</sup>22 °C represents ambient laboratory temperature.

**Table 2. Simulant components and concentrations (Molarity) for selected samples.**

Sample Identification	Simulant <sup>2</sup>	50 wt% NaOH	NaNO <sub>3</sub>	NaNO <sub>2</sub>	Na <sub>2</sub> CO <sub>3</sub>	Na <sub>2</sub> SO <sub>4</sub>	Aluminum Nitrate (9 H <sub>2</sub> O)	Sodium Phosphate (12 H <sub>2</sub> O)
DDA-PA <sup>1</sup>	DDA	0.769	2.202	0.110	0.145	0.044	0.071	0.008
MCU-PA <sup>1</sup>	MCU	1.594	3.159	0.368	0.176	0.059	0.054	0.012
SWPF-PA <sup>1</sup>	SWPF	2.866	1.973	0.485	0.118	0.055	0.114	0.007
GVS-88	SWPF	2.368	2.374	0.580	0.118	0.055	0.114	0.007
GVS-93	SWPF	4.705	1.371	0.583	0.118	0.055	0.449	0.007
GVS-94	SWPF	3.705	0.568	0.386	0.118	0.055	0.449	0.007
GVS-100-01	SWPF	3.535	1.128	0.484	0.118	0.055	0.282	0.007
GVS-100-02	SWPF	3.535	1.128	0.484	0.118	0.055	0.282	0.007
GVS-107	MCU	2.000	1.700	0.550	0.176	0.059	0.220	0.012
GVS-110	MCU	2.680	1.700	0.550	0.176	0.059	0.220	0.012
GVS-111	MCU	2.680	1.700	0.550	0.176	0.059	0.220	0.012
GVS-114	MCU	2.680	1.700	0.550	0.176	0.059	0.220	0.012
GVS-118	MCU	2.680	1.700	0.550	0.176	0.059	0.220	0.012
GVS-121	SWPF	3.810	NA	NA	0.118	NA	0.350	0.007
GVS-123	SWPF	4.610	NA	NA	0.118	NA	0.550	0.007
TR-419	MCU	1.594	3.159	0.368	0.176	0.059	0.540	0.012
TR-503	MCU	1.594	3.159	0.368	0.176	0.059	0.540	0.012
TR-513 <sup>1</sup>	SWPF	2.866	1.973	0.485	0.118	0.055	0.114	0.007
TR-517	MCU	1.594	3.159	0.368	0.176	0.059	0.540	0.012
TR-531 <sup>1</sup>	DDA	0.769	2.202	0.110	0.145	0.044	0.071	0.008
TR-614	MCU	2.680	1.700	0.550	0.176	0.059	0.220	0.024
TR-616	MCU	2.680	1.700	0.550	0.176	0.059	0.220	0.024
TP-006-003	Tank 50	2.920	1.520	0.550	0.176	0.059	0.280	0.012
TP-006-004	Tank 50	2.920	1.520	0.550	0.176	0.059	0.280	0.012
TP-006-005	Tank 50	2.920	1.520	0.550	0.176	0.059	0.280	0.012

<sup>1</sup>Assumed PA projection (NB Grout Variability # 5 page 83)<sup>2</sup>Variations of SWPF, MCU, or DDA simulant.**Table 3. Sample heating profiles.**

Sample Identification <sup>1</sup>	Max Controlled Cure Temp	Heating Profile
GVS-88	60 °C	Isothermal at 60 °C for 1 day
GVS-100-02	60 °C	Isothermal at 60 °C for 28 days
TR-517	40 °C	Isothermal at 40 °C for 7 days
TR-616	40 °C	Isothermal at 40 °C for 1 day
TP-006-003	41 °C	Ramped to 41.1 °C over 3 days
TP-006-004	48 °C	Ramped to 47.9 °C over 4 days
TP-006-005	57 °C	Ramped to 56.4 °C over 5 days

Sorption experiments were performed in air to acquire distribution coefficients ( $K_d$ ) for the measurable elements present in the solid and aqueous leachate at equilibrium. Approximately 0.5 grams of the sample were ground using a mortar and pestle and then added to 7 mL of a saturated  $\text{Ca}(\text{OH})_2$  solution for each leaching experiment. Leach solutions were contacted with the solid for 7 or more days (7-26 d) and subsequently filtered using a 0.45  $\mu\text{m}$  filter.

$K_d$  values (mL/g) were calculated from measurements of the quantity of material in the solids and the quantity of material in the liquids.

$$K_d = \frac{(C_i - C_f) \times V}{C_f \times m_{\text{solids}}} \quad (1)$$

where  $C_i$  is the aqueous activities of the initial (from the “no solids” controls) and  $C_f$  is the final equilibrium activity of each radionuclide (dpm/mL);  $V$  = volume of liquid in the final equilibrated suspension (mL); and  $m_{\text{solids}}$  is the solids mass (g).  $C_i$  and  $C_f$  values of the gamma emitting radionuclides.

A Portlandite ( $\text{Ca}(\text{OH})_2$ ) saturated leaching solution was used in the desorption tests to simulate young and moderately aged cementitious materials<sup>1</sup>, defined in Kaplan 2010. During this cement aging stage,  $\text{Ca}(\text{OH})_2$  and calcium-silicate-hydrate gels are the key solid phases controlling aqueous leachate chemistry (Berner 1992), because  $\text{CO}_2$  in air is very soluble in water at high pH, the resulting dissolved carbonate ( $\text{CO}_3^{2-}$ ) will precipitate as calcite ( $\text{CaCO}_3$ ) in the  $\text{Ca}(\text{OH})_2$  saturated solution. The pH of a  $\text{Ca}(\text{OH})_2$  saturated solution is approximately 12.5. Deionized (DI) water was used for the preparation of  $\text{Ca}(\text{OH})_2$ -saturated solutions. Approximately 20 g of reagent grade  $\text{Ca}(\text{OH})_2$  was added to 2 liters of DI water and stirred for one day. The solution was subsequently filtered using a 0.45  $\mu\text{m}$  filter.

### 3.2 MATERIALS AND METHODS

Saltstone samples were made with simulants of non-radioactive solutions based on projections at the time of DDA, MCU, and SWPF DSS, and Tank 50 analysis (Table 1). Recipes and formulations are presented in detail in Appendix A. Premix was acquired as part of a delivery of cementitious materials to Saltstone used at the SDF (Harbour et al. 2009).

The following is a brief description of the materials and methods used to obtain  $K_d$  values for the cementitious materials measured in air.

<sup>1</sup> The age of the cementitious material varies with the number of pore volumes that passes through the material and “ages” the material (Berner 1992). “Young cementitious materials” may last 1 to 100 pore volumes. In the past, PAs have assumed 50 pore volumes. They have mineral assemblages that produce a aqueous pH of >12, Moderately aged cementitious solids, produce a aqueous phase of pH ~12 and lasts between 100 and 1000 pore volumes. Kaplan 2010 made calculations demonstrating cementitious materials longevity of this stage lasted 500 pore volumes. The third and final cementitious age can last between 1000 and 10,000 pore volumes

### 3.2.1 Materials - Cementitious Materials

- Archived cementitious samples.
- Portlandite ( $\text{Ca}(\text{OH})_2$ ) saturated leaching solution
- $^{137}\text{Cs}$ ,  $^{85}\text{Sr}$ ,  $^{152}\text{Eu}$ , and  $^{129}\text{I}$  isotopes
- Hammer and chisel
- Mortar and pestle
- Test tube rotisserie
- pH
- and ORP meter

### 3.2.2 Methods - Cementitious Materials

Saltstone Samples: Twenty-two 10 g subsamples were collected from various existing simulant saltstone samples that reflect variable formulations, some of which may exist or could be expected to exist in the Saltstone facility. Samples were selected based on availability in an effort to obtain a range of saltstone compositions.

Batch Test: Conduct batch tests with ground cementitious samples, three replicates, nominally 0.5 g saltstone: 7 mL saturated  $\text{Ca}(\text{OH})_2$  on the lab bench (or hood). Leach solutions containing radionuclide isotopes were in contact with cementitious material for at least a 7 day contact period. Samples were filtered using a 0.45  $\mu\text{m}$  filter and subsequently analyzed by gamma spectroscopy to determine equilibrium solution concentrations. ‘No solids control’ samples were analyzed to determine initial solution concentrations for experiments with cementitious materials.

A Portlandite saturated leaching solution was prepared for use in the desorption tests to simulate young/moderately aged cement pore solution (Kaplan et al. 2008). DI water was used for the preparation of  $\text{Ca}(\text{OH})_2$ -saturated solutions. Approximately 20 g of reagent grade  $\text{Ca}(\text{OH})_2$  was added to 2 liters of DI water and stirred for one day. The solution was subsequently filtered using a 0.45  $\mu\text{m}$  filter.

All tests were conducted in triplicate. A positive control was included with each set of experiments; ‘no-solids’ control samples were used to determine if precipitation of the radionuclides occurred during the experiments.  $K_d$  values of Cs, Sr, and I were calculated using Equation 1, which calculates sorption by subtracting the concentration of radionuclide added from the concentration remaining in solution at the end of the one-week or greater equilibration period. All AD data is archived in the Analytical Development’s LIMS system.

To set up the leaching experiments, nominally 0.5 g amounts of the ground cementitious materials were each added to a clean 15 mL centrifuge tube for each test, and labeled with the identification of the sample. Experiments were run in triplicate. The solution phase was held constant for all sorption experiments and contacted with the solids for 7- 28 days. For each experiment, centrifuge tube was continuously rotated on a rotisserie during the contact period. The solutions were subsequently filtered using a 0.45  $\mu\text{m}$  filter. Approximately 4 mL of each

solution was submitted to AD for analysis of final radionuclide concentration. The initial spike concentration was determined by using the data from the no-solids control sample.

### 3.2.3 Materials and Methods - Soil Samples

Selection of Sediment Pu  $K_d$  Values from the Literature: Selection of Pu  $K_d$  values from the literature had to meet the following criteria; that is they had to be measured in:

- SRS sediment,
- In pH 4.6 to 7.0,
- Been spiked with Pu(IV) or Pu(V)
- If spiked with Pu(V), the Pu(V) had to have contact with the soil greater than 2 days (to permit Pu(V) reduction to Pu(IV) (Kaplan, 2006) (Powell, 2002a)). This minimum of two days of contact time was selected based on careful oxidation state characterization experimentation and approach to equilibration experimentation conducted on SRS sediments (Kaplan et al., 2004; Powell, 2002b). In short, once Pu(V) comes in contact with SRS sediments, even under bench top conditions, it undergoes near complete reduction to Pu(IV) within 30 hr; Pu(V) concentration decrease and ingrowth of Pu(IV) increases in the aqueous phase and solid phase. After one day of contact, Pu(V)  $K_d$  values were one to three orders of magnitude lower than Pu(IV)  $K_d$  values added to the same sediment. Within 33 days,  $K_d$  values of the Pu(V) spiked samples had increased to the same levels as those of the Pu(IV) spiked samples. Some of these kinetic oxidation transformation trends and approach to steady state conditions are demonstrated in the data presented in Appendix B.

Furthermore, to estimate the range and distribution of  $K_d$  values in a cementitious leachate passing through sediment the above selection criteria were used, except:

- the acceptable pH criteria were expanded to 4.6 to 11.0.

The average pH of SRS aquifer groundwater is ~5.5 (Kaplan, 2010).

The soil type, pH,  $K_d$ , Pu contact time, reference, and oxidation state of the Pu spike are presented in Table 12. Pu  $K_d$  values selected from the literature used to develop the Pu  $K_d$  sediment distribution (sorted by pH). The properties of the sediments used in the Pu  $K_d$  measurements selected are presented in Table 13.

### 3.2.4 Statistical Approach – Distribution Model Comparisons

Eleven different models were evaluated for their ability to fit the  $K_d$  value distributions. They included the Frechet, generalized Gamma, loglogistic, lognormal, log Generalized Gamma, Weibull, Exponential, LEV, logistic, Normal, and SEV; they are defined in the software JMP (SAS Cary, NC). The approach for selecting the appropriate distribution model was to first do statistical analyses through the use of three goodness-of-fit test: AIC: Akaike information criterion; BIC: Schwartz's Bayesian information criterion; -2 log likelihood: -2 times the natural



log of the likelihood evaluated with the best-fit estimates of the parameters). One can obtain a rather simple and quick understanding of these parameters through a WIKIPEDIA search of "Akaike information criterion" and a more detailed description can be found in Claeskens and Hjort (2008). Each of these goodness-of-fit tests provided slightly different information about how well the estimated distribution models fit the actual  $K_d$  distributions, i.e., they are tools for model selection, they rank models.<sup>2</sup> Then the actual distributions were plotted and they were inspected to make sure that the *general* fit that was represented by the goodness-of-fit, capture the more salient aspects of the dataset, including the low  $K_d$  as well as the high  $K_d$  values (as opposed, for example, only capturing the midrange- and high-  $K_d$  data). The goodness-of-fit provides a measure that is appropriate for ranking however it does not tell you if the fit is adequate for a specific application. Then finally, we evaluated whether there was a consistency with a given distribution model, suggesting that a general consistency may exist through a phenomenological process in the data set. The intent was to assign as few distributions as possible and if multiple distributions are assigned, assign them with different populations in mind. The stochastic modeling conducted in Goldsim includes an entire distribution, which include  $2\sigma$  or 95% confidence.

## 4.0 RESULTS AND DISCUSSION

$K_d$  values include not only adsorption and absorption mechanisms, but can also reflect precipitation. Some precipitation of the radionuclides may have occurred because control samples where aqueous radionuclide concentration decreases were observed in the absence of added solids. Precipitation or adsorption to test vessel walls of Eu precluded the ability to calculate  $K_d$  values. Eu concentrations were below detection limits for no-solid controls and all samples containing cementitious solids. Therefore the measured decreases in aqueous radionuclides were due to causes other than the sorption of the radionuclides by the added solid phases.

In Table 4 calculated  $K_d$  values are presented for Cs, Sr, and I for each replicate (A, B, C) and the average of the three replicates. A discussion of results by element follows.

---

<sup>2</sup> As a rough rule of thumb, models having their AIC within 1–2 of the minimum have substantial support and should receive consideration in making inferences. Models having their AIC within about 4–7 of the minimum have considerably less support, while models with their AIC > 10 above the minimum have either essentially no support and might be omitted from further consideration or at least fail to explain some substantial structural variation in the data - Akaike, Hirotugu (1980). "Likelihood and the Bayes procedure", *Bayesian Statistics*, Ed. J. M. Bernardo *et al.*, Valencia: University Press. p.143-166.

**Table 4 .  $K_d$  values (mL/g) calculated from adsorption experiments for cesium, strontium, and iodine.**

Sample ID	Cesium ( $K_d$ )				Strontium ( $K_d$ )				Iodine ( $K_d$ )			
	A	B	C	Average $K_d$ (ABC)	A	B	C	Average $K_d$ (ABC)	D	E	F	Average $K_d$ (DEF)
GVS-88	436	310	363	370	4801	3501	6938	5080	0.8	-0.1	0.4	0.4
GVS-93	12	19	13	15	341	361	364	355	5.1	1.4	2.5	3.0
GVS-94	19	24	24	22	539	429	448	472	-0.4	1.2	1.8	0.9
GVS-100-01	22	20	22	21	853	613	961	809	2.0	1.0	1.7	1.5
GVS-100-02	293	173	160	208	1817	1529	1710	1685	0.6	1.0	3.4	1.7
GVS-107	66	75	85	75	571	634	570	592	NM	1.5	-0.9	0.3
GVS-110	21	16	16	18	455	598	537	530	2.0	2.2	2.5	2.2
GVS-111	19	19	20	19	711	733	709	718	0.7	3.2	3.5	2.5
GVS-114	13	14	15	14	364	428	451	414	2.7	2.9	2.9	2.9
GVS-118	19	11	12	14	581	301	272	385	0.6	1.5	0.1	0.7
GVS-121	32	32	33	33	929	840	1339	1036	3.4	0.9	-0.2	1.4
GVS-123	17	26	27	23	736	612	1045	798	2.5	-0.6	0.2	0.7
TR-419	14	14	12	13	602	417	613	544	-1.1	0.4	0.3	-0.1 <sup>1</sup>
TR-503	12	19	19	16	335	327	309	323	0.8	0.5	0.9	0.7
TR-513	24	23	21	22	317	381	492	397	-0.9	0.5	0.0	-0.1 <sup>1</sup>
TR-517	17	14	11	14	293	279	260	277	0.6	3.9	1.9	2.1
TR-531	17	15	9	14	132	122	138	131	-0.6	-0.2	0.6	-0.1 <sup>1</sup>
TR-614	9	7	7	8	228	202	216	216	-0.1	0.9	0.0	0.3
TR-616	26	44	37	36	1044	956	828	943	0.5	1.9	0.9	1.1
TP-006-003	5	6	8	6	475	484	490	483	-0.5	0.6	-0.7	-0.2 <sup>1</sup>
TP-006-004	9	9	9	9	406	400	388	398	-1.5	0.6	0.7	-0.1 <sup>1</sup>
TP-006-005	8	11	6	8	715	704	658	692	-1.4	1.0	4.2	1.3

<sup>1</sup>ion concentration at steady-state was higher than control experiment

NM = not measured

Standard deviation of each average and standard deviation of the three replicates is provided in Appendix A.

**Table 5. Previously reported  $K_d$  values for cementitious materials under oxidizing and reducing conditions.**

Element	Best Oxidizing Cement $K_d$ Young	Best Oxidizing Cement $K_d$ Middle	Best Oxidizing Cement $K_d$ Old	Best Reducing Cement $K_d$ Young	Best Reducing Cement $K_d$ Middle	Best Reducing Cement $K_d$ Old
Cs	2	20	10	2	20	10
Sr	15	15	5	15	15	5
I	8	15	4	5	9	4

SRNL-STI-2009-00473

## 4.1 CESIUM MEASURED IN CEMENTITIOUS MATERIALS

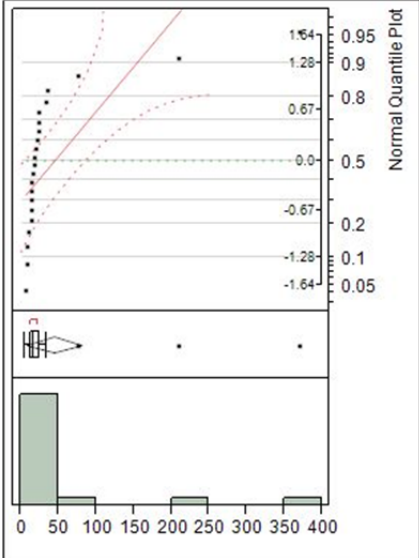
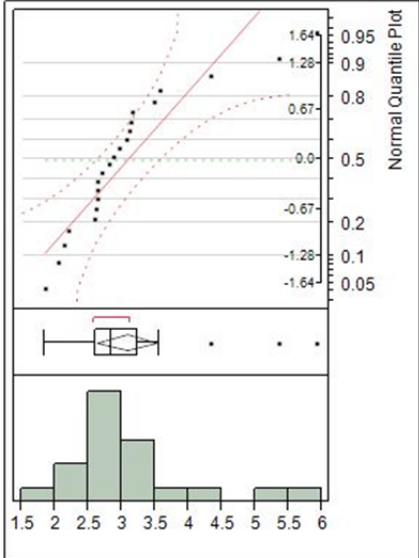
The Cs  $K_d$  values ranged from 6.3 to 370 mL/g and the mean was  $44.5 \pm 84$  mL/g (Table 6) in this test and are compared with reported values of 2 and 20 for young and middle cement, respectively (Table 6) (Kaplan 2009). This experimentally derived range is extremely wide, wider than the mean; coefficient of variation is 189% ( $CV = \text{standard deviation}/\text{mean} \times 100$ ); Table 6). The wide range of  $K_d$  values obtained was in part the result of the range of recipes used to make the saltstone (varying simulant, premix ratios, water to premix, aluminate, temperature curing, sample age). This range of condition was selected to approximate conditions that may exist under field conditions, where mixing may be difficult to control. In closer statistical examination of the data, much of this variance can be attributed to two data, GVW-88 ( $K_d$  370 mL/g) and GVS-100-02 ( $K_d$  = 208 mL/g); both these samples were heat treated to 60 °C (Table 3 and 4). This was further evaluated statistically by asking if these two data represent another population, i.e., if these two data points are outliers (see the 2-component normal fit to the Cs distribution data in Appendix A; Table 26). There was not sufficient data to demonstrate a separate population, but a trend appears. Furthermore, regression analysis between temperature (Table 3 and 4) and Cs  $K_d$  resulted in a significant correlation ( $r = 0.59$ ; significant at  $P \leq 0.05$ ). The regression was strongly driven by the two points and was not a continuous trend. When the Cs  $K_d$  values were categorized by temperature, again there appeared to be an indication of temperature dependence on Cs  $K_d$  values:

- all data  $K_d = 45 \pm 84$  mL/g ( $n = 22$ );
- 60°C  $K_d = 289 \pm 115$  mL/g ( $n = 2$ );
- <60°C  $K_d = 20 \pm 15$  mL/g ( $n = 20$ );
- 22°C  $K_d = 18 \pm 15$  mL/g ( $n = 15$ )

Additional related statistics are in Appendix A. It is anticipated that upon further research the influence of temperature effect on sorption will be better understood and the range of values will be greatly contracted. At present, the full range of temperature conditions at the saltstone facility are not fully known and the impact of curing temperature on cement-phase mineral formation and subsequent radionuclide sorption. This is discussed in more detail in Section 4.5.

In the literature, Cs  $K_d$  values in hardened HTS cement discs (Haute Teneur en Silice, a French sulphate resistant cement), pH 13.3 were close to 3 mL/g (Sarott et al. 1992). Wieland and Van Loon (2003) reviewed Cs  $K_d$  values of various cementitious materials and they had a very narrow range of 0.2 to 5 mL/g. Kaplan and Coates (2007) measured cesium  $K_d$  values in  $\text{Ca}(\text{OH})_2$ -saturated and  $\text{Ca-CaCO}_3$ -saturated solutions in ground, 40-year old concrete, simulating 1<sup>st</sup>/2<sup>nd</sup> and 3<sup>rd</sup> Stages, respectively. Measured  $K_d$  values were 21, and 17.6 mL/g, respectively.

Table 6. Plots and descriptive statistics for Cs  $K_d$  values in saltstone

Distribution of the Mean(Cs- $K_d$ )			Distribution of the Log <sub>e</sub> (Mean(Cs- $K_d$ ))		
					
<b>Quantiles</b> 100.0%      maximum                      369.667 99.5%    369.667 97.5%    369.667 90.0%    168.667 75.0%          quartile                      25.5833 50.0%          median                        17.1667 25.0%          quartile                      13.5833 10.0%    7.86667 2.5%    6.33333 0.5%    6.33333 0.0%          minimum                      6.33333			<b>Quantiles</b> 100.0%      maximum                      5.9126 99.5%    5.9126 97.5%    5.9126 90.0%    5.03509 75.0%          quartile                      3.23144 50.0%          median                        2.84255 25.0%          quartile                      2.60879 10.0%    2.0619 2.5%    1.84583 0.5%    1.84583 0.0%          minimum                      1.84583		
<b>Moments</b> Mean    44.545455 Std Dev    84.212351 Std Err Mean                                    17.954134 Upper 95% Mean                              81.883119 Lower 95% Mean                              7.2077898 N    22 Variance     7091.7201 Skewness     3.3630383 Kurtosis    11.540562 CV    189.04813 N Missing     0			<b>Moments</b> Mean    3.0780819 Std Dev    0.9933274 Std Err Mean                                    0.2117781 Upper 95% Mean                              3.5184986 Lower 95% Mean                              2.6376652 N    22 Variance     0.9866994 Skewness     1.6753091 Kurtosis    2.9279735 CV    32.270988 N Missing     0		

The data distribution in Table 6 also demonstrates that the Cs  $K_d$  are clearly not normally distributed, especially when one looks at the “Distribution of the Mean(Cs- $K_d$ )” data on the left in Table 6. The **skewness** value is a measure of the asymmetry of the probability distribution of a real-valued random variable. The positive skewness value means it tails to the right as shown in Table 6. The relatively large value ( $>3.0$ ) of 3.36, suggest that the right tail is much longer than the left tail and that a normal distribution is not appropriate. Like skewness, kurtosis, is used to describe the probability distribution. **Kurtosis** is a measure of the “peakedness” of the

probability distribution. In Table 6, the kurtosis is relatively large value, suggesting a spreading of the distribution, as oppose to forming a sharp peak. Again, there are no other reported distributions of cementitious  $K_d$  values in the literature to compare these statistics.

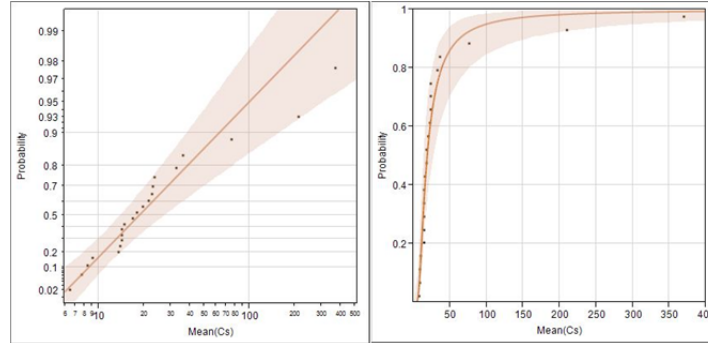
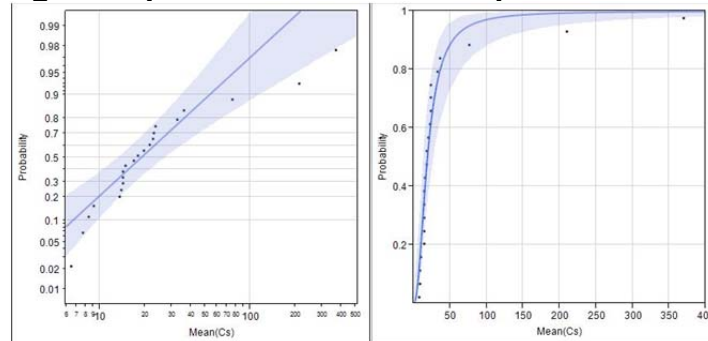
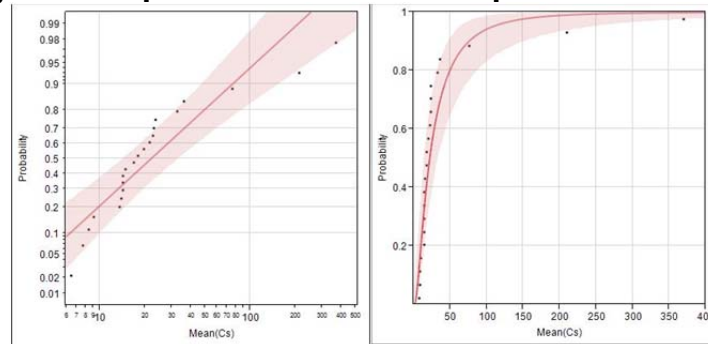
#### 4.1.1 Cesium $K_d$ Model Comparisons of Distribution Fits:

Goodness of fit analysis of the 12 distribution models (discussed in Section 3.2.4) indicated that the (from best fit to worse fit) Frechet, Generalized Gamma, Loglogistic, and Lognormal distribution models had the best fit. Lower the goodness of fit value, the better the fit. Not surprising the normal distribution was not representative of the dataset (Table 6). The Frechet and Loglogistic distributions are presented in Figure 1. (The Generalized Gamma model was not considered when more simple models are available; it has a third fitting parameters, when the others generally only require two fitting parameters.) Frechet model is best on two of three global metrics. Extended Generalized Gamma does best on likelihood.

**Table 7. Goodness-of-fit of distribution models for Cs  $K_d$  values in saltstone.**

<b>Distribution</b>	<b>AICc<sup>a</sup></b>	<b>-2Loglikelihood</b>	<b>BIC</b>
Frechet	192.32093	187.68936	193.87144
Generalized Gamma	194.02134	186.68801	195.96113
Loglogistic	197.89614	193.26456	199.44664
Lognormal	201.18246	196.55088	202.73297
Log Generalized Gamma	212.33922	205.00589	214.27902
Weibull	213.01320	208.38162	214.56370
Exponential	213.24645	211.04645	214.13749
LEV	233.58784	228.95627	235.13835
Logistic	247.30243	242.67085	248.85293
Normal	261.10846	256.47689	262.65897
SEV	279.85554	275.22396	281.40604

<sup>a</sup> AIC: Akaike information criterion; BIC: Schwartz's Bayesian information criterion; -2 log likelihood: -2 times the natural log of the likelihood evaluated with the best-fit estimates of the parameters

**Frechet: quantile on left and nonparametric on right****Loglogistic: quantile on left and nonparametric on right****Lognormal: quantile on left and nonparametric on right**

**Figure 1.** (TOP) The Frechet distribution of the Cs  $K_d$  Saltstone data set. Plot on left (quantile) is a linear version of plot on right (nonparametric). Shaded region provides 95% confidence region. Note no points outside shaded zone. Frechet distribution fits the low- and mid  $K_d$  values especially well. (MIDDLE) The Loglogistic distribution of the Cs  $K_d$  saltstone data set quantile (left) and nonparametric (right). Note that there are three or four data points outside the shaded region and the low  $K_d$  fit is poor even though the general goodness-of-fit is very acceptable. (BOTTOM) Lognormal distribution of Cs  $K_d$  saltstone data set quantile (left and nonparametric (right) Of the three models, this one is the poorest.

## 4.2 STRONTIUM $K_d$ VALUES MEASURED IN CEMENTITIOUS MATERIALS

The Sr  $K_d$  values ranged from 131 to 5080 and had a mean of  $785 \pm 1016$  (Table 8). Again, the distribution is extremely large, greater than the mean, with a coefficient of variation (standard deviation/mean  $\times 100$ ) of 129%. Like the distribution of the Cs  $K_d$  values, this wide variation appears to stem primarily from one or at most three samples. This is easiest seen in the histogram of the data distribution in Table 8. Looking at the individual data points in Table 4 the three largest  $K_d$  values were from sample GVS-88 ( $K_d = 5080$  mL/g), GVS-100-02 ( $K_d = 1685$  mL/g) and GVS-121 (1036 mL/g); the first two had some form of a 60° C heat treatment (Table 3). The values reported here are more in line with those reported in desorption experiments with actual saltstone sample recovered from the Saltstone Facility (Almond and Kaplan 2011). Those samples, in which the Sr was desorbed under oxidizing and reducing conditions, resulted in apparent  $K_d$  values of 737 and 5728 mL/g. These higher  $K_d$  values were attributed to the potential formation of Sr-sulfate phases and it was supported by the high apparent  $K_d$  under oxidizing than reducing conditions.

The currently reported  $K_d$  value for strontium in young and middle aged cementitious environments is identical, 15 mL/g (Table 5; Kaplan 2010).. Strontium typically has a moderately low  $K_d$  in cementitious environments; however, when sulfate concentrations are high,  $\text{SrSO}_4$  precipitates, as was likely the case here.  $\text{SrSO}_4$  has a solubility of  $3.2\text{E-}07$  M (strontium sulfite solubility product is even lower,  $\text{SrSO}_3 K_{sp} = 4\text{E-}08$  M). Large Sr sorption was also noted under reducing conditions.

Jakubick et al. (1987) reported Sr  $K_d$  values of 0.8 to 1.6 mL/g for high density and normal density concretes, and 1.3 to 3 mL/g for the same concretes, but in lower ionic strength solutions. Ewart et al. (1986) reported  $K_d$  values between 1 and 4 mL/g. Kato and Yanase (1993) reported a Sr  $K_d$  value of 56 mL/g for an experiment involving 24 h contact time, dried cement powder, pH 11 cement equilibrated water. Previously, we elected to disregard this value because it is an order-of-magnitude greater than those reported by other researchers and the nature of the solid phase was not clearly described by the author. In 1<sup>st</sup> Stage  $K_d$  values were decreased because high ionic strength likely results in competitive exchange (desorption). Kaplan and Coates (2007) measured Sr  $K_d$  values in  $\text{Ca(OH)}$ -saturated and  $\text{CaCO}_3$ -saturated solutions in ground, 40-yr old concrete, simulating 1<sup>st</sup>/2<sup>nd</sup> and 3<sup>rd</sup> Stages, respectively. The measured  $K_d$  values were 28.1 and 39.1 mL/g, respectively.

Table 8. Plots and descriptive statistics for Sr  $K_d$  values in saltstone

Distribution of the Mean(Sr-K <sub>d</sub> )	Distribution of the Log(Mean(Sr-K <sub>d</sub> ))																																																																		
<p>The plot shows a normal quantile plot with data points following a red normal distribution line. Below it is a histogram of the mean values, showing a right-skewed distribution with a peak around 500 and a tail extending to 5000.</p>	<p>The plot shows a normal quantile plot with data points following a red normal distribution line. Below it is a histogram of the log-transformed mean values, showing a more symmetric distribution with a peak around 0.5 and a tail extending to 5.0.</p>																																																																		
<b>Quantiles</b> <table><tr><td>100.0%</td><td>maximum</td><td>5,080</td></tr><tr><td>99.5%</td><td></td><td>5,080</td></tr><tr><td>97.5%</td><td></td><td>5,080</td></tr><tr><td>90.0%</td><td></td><td>1490.53</td></tr><tr><td>75.0%</td><td>quartile</td><td>800.5</td></tr><tr><td>50.0%</td><td>median</td><td>506.5</td></tr><tr><td>25.0%</td><td>quartile</td><td>377.333</td></tr><tr><td>10.0%</td><td></td><td>233.933</td></tr><tr><td>2.5%</td><td></td><td>130.667</td></tr><tr><td>0.5%</td><td></td><td>130.667</td></tr><tr><td>0.0%</td><td>minimum</td><td>130.667</td></tr></table>	100.0%	maximum	5,080	99.5%		5,080	97.5%		5,080	90.0%		1490.53	75.0%	quartile	800.5	50.0%	median	506.5	25.0%	quartile	377.333	10.0%		233.933	2.5%		130.667	0.5%		130.667	0.0%	minimum	130.667	<b>Quantiles</b> <table><tr><td>100.0%</td><td>maximum</td><td>8.53307</td></tr><tr><td>99.5%</td><td></td><td>8.53307</td></tr><tr><td>97.5%</td><td></td><td>8.53307</td></tr><tr><td>90.0%</td><td></td><td>7.28374</td></tr><tr><td>75.0%</td><td>quartile</td><td>6.68522</td></tr><tr><td>50.0%</td><td>median</td><td>6.22645</td></tr><tr><td>25.0%</td><td>quartile</td><td>5.93255</td></tr><tr><td>10.0%</td><td></td><td>5.4481</td></tr><tr><td>2.5%</td><td></td><td>4.87265</td></tr><tr><td>0.5%</td><td></td><td>4.87265</td></tr><tr><td>0.0%</td><td>minimum</td><td>4.87265</td></tr></table>	100.0%	maximum	8.53307	99.5%		8.53307	97.5%		8.53307	90.0%		7.28374	75.0%	quartile	6.68522	50.0%	median	6.22645	25.0%	quartile	5.93255	10.0%		5.4481	2.5%		4.87265	0.5%		4.87265	0.0%	minimum	4.87265
100.0%	maximum	5,080																																																																	
99.5%		5,080																																																																	
97.5%		5,080																																																																	
90.0%		1490.53																																																																	
75.0%	quartile	800.5																																																																	
50.0%	median	506.5																																																																	
25.0%	quartile	377.333																																																																	
10.0%		233.933																																																																	
2.5%		130.667																																																																	
0.5%		130.667																																																																	
0.0%	minimum	130.667																																																																	
100.0%	maximum	8.53307																																																																	
99.5%		8.53307																																																																	
97.5%		8.53307																																																																	
90.0%		7.28374																																																																	
75.0%	quartile	6.68522																																																																	
50.0%	median	6.22645																																																																	
25.0%	quartile	5.93255																																																																	
10.0%		5.4481																																																																	
2.5%		4.87265																																																																	
0.5%		4.87265																																																																	
0.0%	minimum	4.87265																																																																	
<b>Moments</b> <table><tr><td>Mean</td><td>785.33333</td></tr><tr><td>Std Dev</td><td>1016.8829</td></tr><tr><td>Std Err Mean</td><td>216.80017</td></tr><tr><td>Upper 95% Mean</td><td>1,236.194</td></tr><tr><td>Lower 95% Mean</td><td>334.4727</td></tr><tr><td>N</td><td>22</td></tr><tr><td>Variance</td><td>1034050.9</td></tr><tr><td>Skewness</td><td>3.9282015</td></tr><tr><td>Kurtosis</td><td>16.76389</td></tr><tr><td>CV</td><td>129.48424</td></tr><tr><td>N Missing</td><td>0</td></tr></table>	Mean	785.33333	Std Dev	1016.8829	Std Err Mean	216.80017	Upper 95% Mean	1,236.194	Lower 95% Mean	334.4727	N	22	Variance	1034050.9	Skewness	3.9282015	Kurtosis	16.76389	CV	129.48424	N Missing	0	<b>Moments</b> <table><tr><td>Mean</td><td>6.3186987</td></tr><tr><td>Std Dev</td><td>0.744799</td></tr><tr><td>Std Err Mean</td><td>0.1587917</td></tr><tr><td>Upper 95% Mean</td><td>6.6489241</td></tr><tr><td>Lower 95% Mean</td><td>5.9884733</td></tr><tr><td>N</td><td>22</td></tr><tr><td>Variance</td><td>0.5547255</td></tr><tr><td>Skewness</td><td>1.0326982</td></tr><tr><td>Kurtosis</td><td>2.9936167</td></tr><tr><td>CV</td><td>11.787221</td></tr><tr><td>N Missing</td><td>0</td></tr></table>	Mean	6.3186987	Std Dev	0.744799	Std Err Mean	0.1587917	Upper 95% Mean	6.6489241	Lower 95% Mean	5.9884733	N	22	Variance	0.5547255	Skewness	1.0326982	Kurtosis	2.9936167	CV	11.787221	N Missing	0																						
Mean	785.33333																																																																		
Std Dev	1016.8829																																																																		
Std Err Mean	216.80017																																																																		
Upper 95% Mean	1,236.194																																																																		
Lower 95% Mean	334.4727																																																																		
N	22																																																																		
Variance	1034050.9																																																																		
Skewness	3.9282015																																																																		
Kurtosis	16.76389																																																																		
CV	129.48424																																																																		
N Missing	0																																																																		
Mean	6.3186987																																																																		
Std Dev	0.744799																																																																		
Std Err Mean	0.1587917																																																																		
Upper 95% Mean	6.6489241																																																																		
Lower 95% Mean	5.9884733																																																																		
N	22																																																																		
Variance	0.5547255																																																																		
Skewness	1.0326982																																																																		
Kurtosis	2.9936167																																																																		
CV	11.787221																																																																		
N Missing	0																																																																		

#### 4.2.1 Strontium $K_d$ Model Comparisons of Distribution Fits

Goodness of fit analysis of the 12 distribution models (Section 3.2.4) indicated that the (from best fit to worse fit) Loglogistic, Frechet, Lognormal, and Generalized Gamma distribution models had the best fit (Table 9). Lower the goodness of fit value, the better the fit. Again, not surprising the normal distribution was not representative of the dataset (Table 8). The Frechet

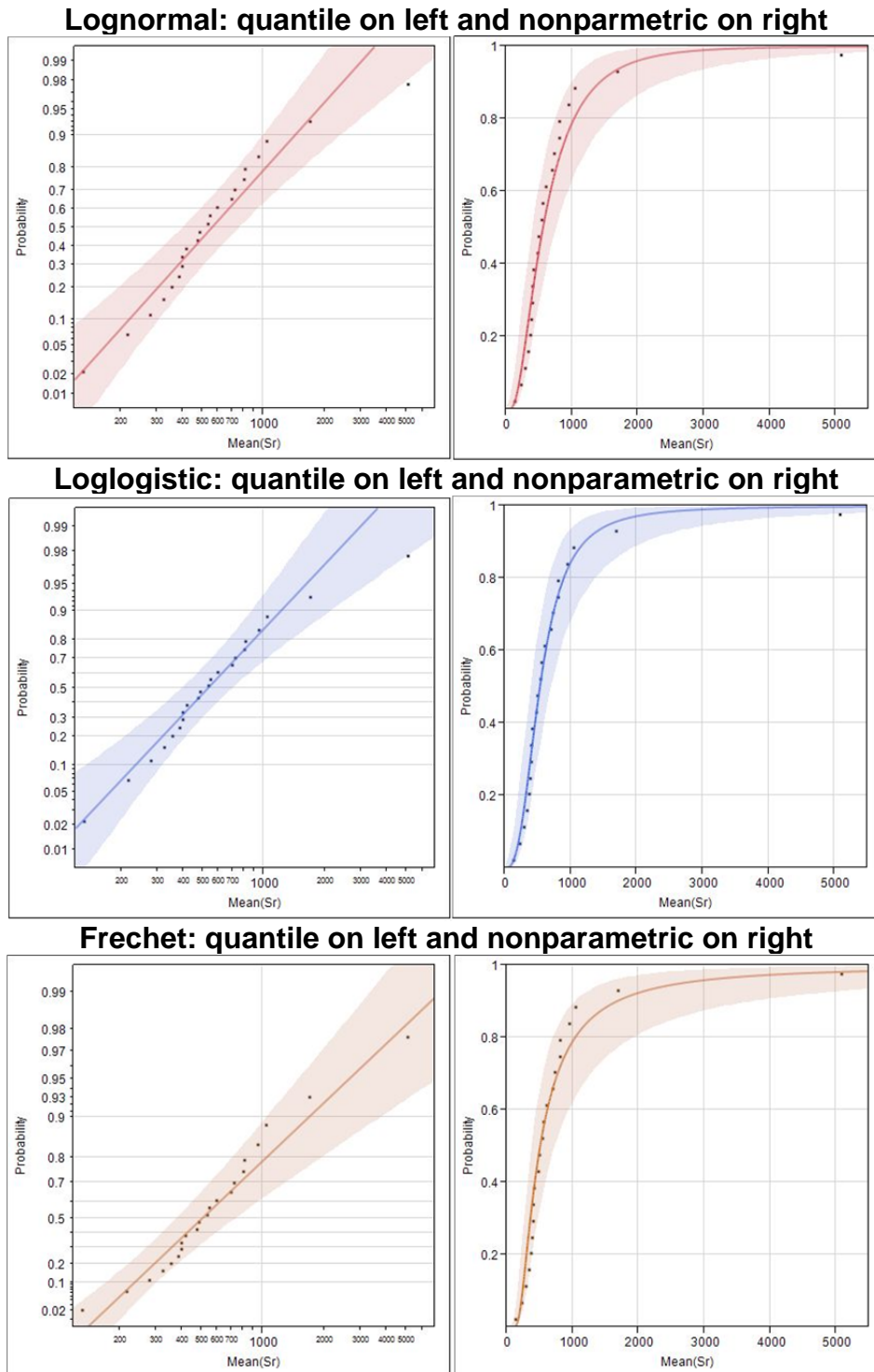


and Loglogistic distributions are presented in Figure 2. The Generalized Gamma model was not considered when more simple models were available; it has a third fitting parameters, whereas the others generally only require two fitting parameters.

**Table 9. Goodness-of-fit of distribution models for Sr  $K_d$  values in saltstone.**

<b>Distribution</b>	<b>AICc<sup>a</sup></b>	<b>-2Loglikelihood</b>	<b>BIC</b>
Loglogistic	328.72148	324.08991	330.27199
Frechet	329.92418	325.29260	331.47469
Lognormal	331.09998	326.46840	332.65048
Generalized Gamma	331.66867	324.33534	333.60846
Log Generalized Gamma	337.12898	329.79564	339.06877
Exponential	339.50876	337.30876	340.39981
Weibull	341.44548	336.81390	342.99598
LEV	343.48815	338.85657	345.03865
Logistic	354.48205	349.85047	356.03255
Normal	370.71931	366.08773	372.26982
SEV	391.75553	387.12395	393.30604

<sup>a</sup> AIC: Akaike information criterion; BIC: Schwartz's Bayesian information criterion; -2 log likelihood: -2 times the natural log of the likelihood evaluated with the best-fit estimates of the parameters  
 Frechet is best on 2 of 3 global metrics. Extended Generalized Gamma does best on likelihood.

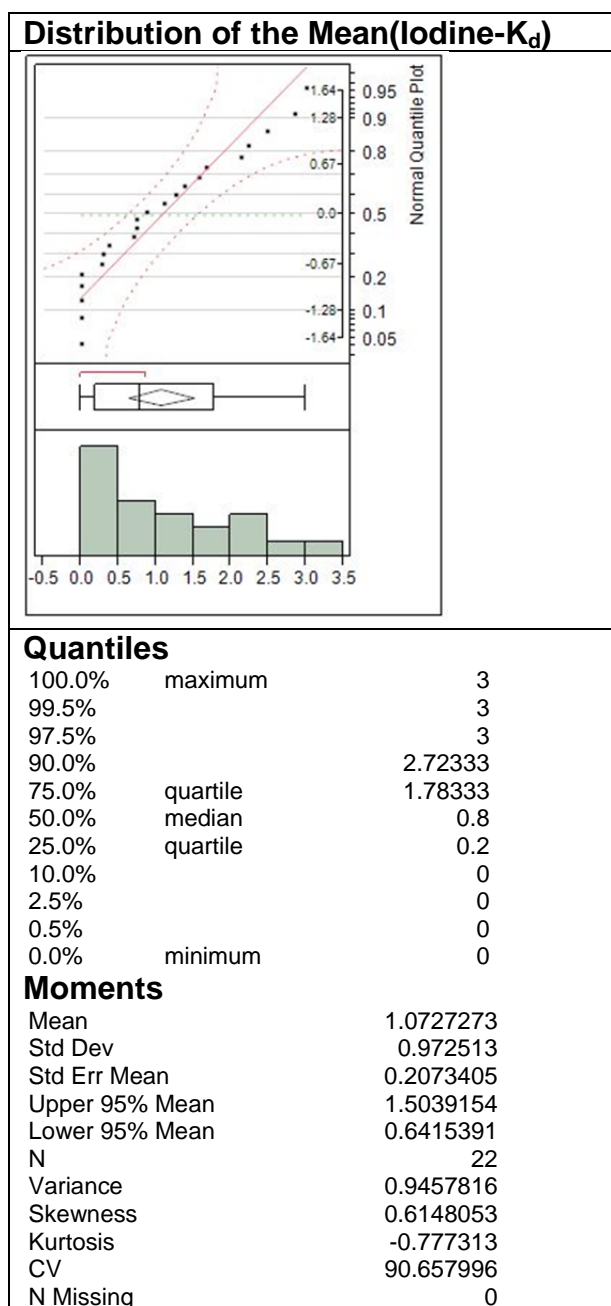


**Figure 2. Lognormal, loglogistic and Frechet quantile and nonparametric plots of the Sr  $K_d$  Saltstone data. Shaded region provides 95% confidence region. Compared to the Frechet, the loglogistic distribution seems to be a bit better than the Frechet for low  $K_d$  values, and near the “elbow” of the graph.**

### 4.3 IODINE MEASURED IN CEMENTITIOUS MATERIALS

The  $K_d$  values ranged from -0.2 to 3.0 (Table 4). But it was decided that the negative  $K_d$  values were not physically meaningful for this system and could not be handled with some of the distribution models. For statistical purposes the negative  $K_d$  values were reassigned to zero values. Our lab has reported anion exclusion, or negative  $K_d$  values to  $\text{TcO}_4^-$  to highly negatively charge sediments (not SRS sediments) (Kaplan and Serne 1998), but this system does not at present support assigning negative  $K_d$  values. The negative  $K_d$  values in Table 4 suggest that the negative  $K_d$  values stems more from analytical uncertainty than from anion exclusion (see samples TR-419, TR-513, TR-531, and TP-006-003). This is acceptable analytical error at these low  $K_d$  values.

The mean iodine  $K_d$  value is  $1.0 \pm 0.97$  mL/g (Table 10). The somewhat narrower standard deviation compared to the Cs and Sr  $K_d$  value measured values is likely real due to the generally low  $K_d$  values as well as to the fact that the  $K_d$  range was artificially truncated at 0 mL/g. The skewness and kurtosis is also low, suggesting that the data is evenly distributed and has a peak (is not flat; these terms are discussed in section 3.2.4.)

Table 10. Plot and descriptive statics for iodine  $K_d$  values in saltstone.

#### 4.3.1 Iodine $K_d$ Model Comparisons of Distribution Fits

One difference with the iodine data was that there were negative values and as mentioned above, it is believed that there is not negative adsorption (anion exclusion) occurring (Table 4).

Negative values in the distribution would require special consideration for distributions. Rather than delete these values from the data set, they were set to zero. The logic was, it is better to

weigh the data set low, then to delete the data and not acknowledge their presence in the dataset. Then distribution model fit analyses were conducted using zero-inflated distributions. This essentially means that there are more zero  $K_d$ 's (realistically small  $K_d$ 's) than one might expect. This surplus of small values does not affect the fit of the distribution to the positive  $K_d$  values and in essence, the distribution treats the fit of the data as if there is two groups of data, the data equal to zero, and the non-zero data. The origin of zero-inflated distributions comes from reliability studies where a certain segment of the population cannot respond or has failed prior to being put on test. In the current case we have selected a surplus of zero  $K_d$  samples.

Four zero-inflated distributions were tried: Weibull, lognormal, loglogistic, and Frechet (Table 11). Here are the goodness-of-fit statistics. Smallest values indicate the best fit to the data. (AIC: Akaike information criterion; BIC: Schwartz's Bayesian information criterion; -2 log likelihood: -2 times the natural log of the likelihood evaluated with the best-fit estimates of the parameters). The zero-inflated Weibull, Lognormal and Loglogistic distribution had reasonably general fits to the data. Only the zero-inflated Weibull distribution seems to fit the data well between the  $K_d$  values of 1 and 2 mL/g. The Weibull is the best for all three global criteria. Note that the fitted line in all cases does not attempt to intercept the data at 0 mL/g; instead the predicted line runs parallel to the x-axis from the last data point ( $K_d \sim 0.3/P \sim 0.22$ ). This low data fit to the data is unique to the zero-inflated distribution models.

**Table 11. Goodness-of-fit of distribution models for iodine  $K_d$  values in saltstone.**

Distribution	AICc <sup>a</sup>	-2Loglikelihood	BIC
Zero Inflated Weibull	50.172673	42.839339	52.112467
Zero Inflated Lognormal	51.760036	44.426703	53.699830
Zero Inflated Loglogistic	52.772682	45.439349	54.712476
Zero Inflated Frechet	55.530240	48.196906	57.470034

<sup>a</sup> AIC: Akaike information criterion; BIC: Schwartz's Bayesian information criterion; -2 log likelihood: -2 times the natural log of the likelihood evaluated with the best-fit estimates of the parameters

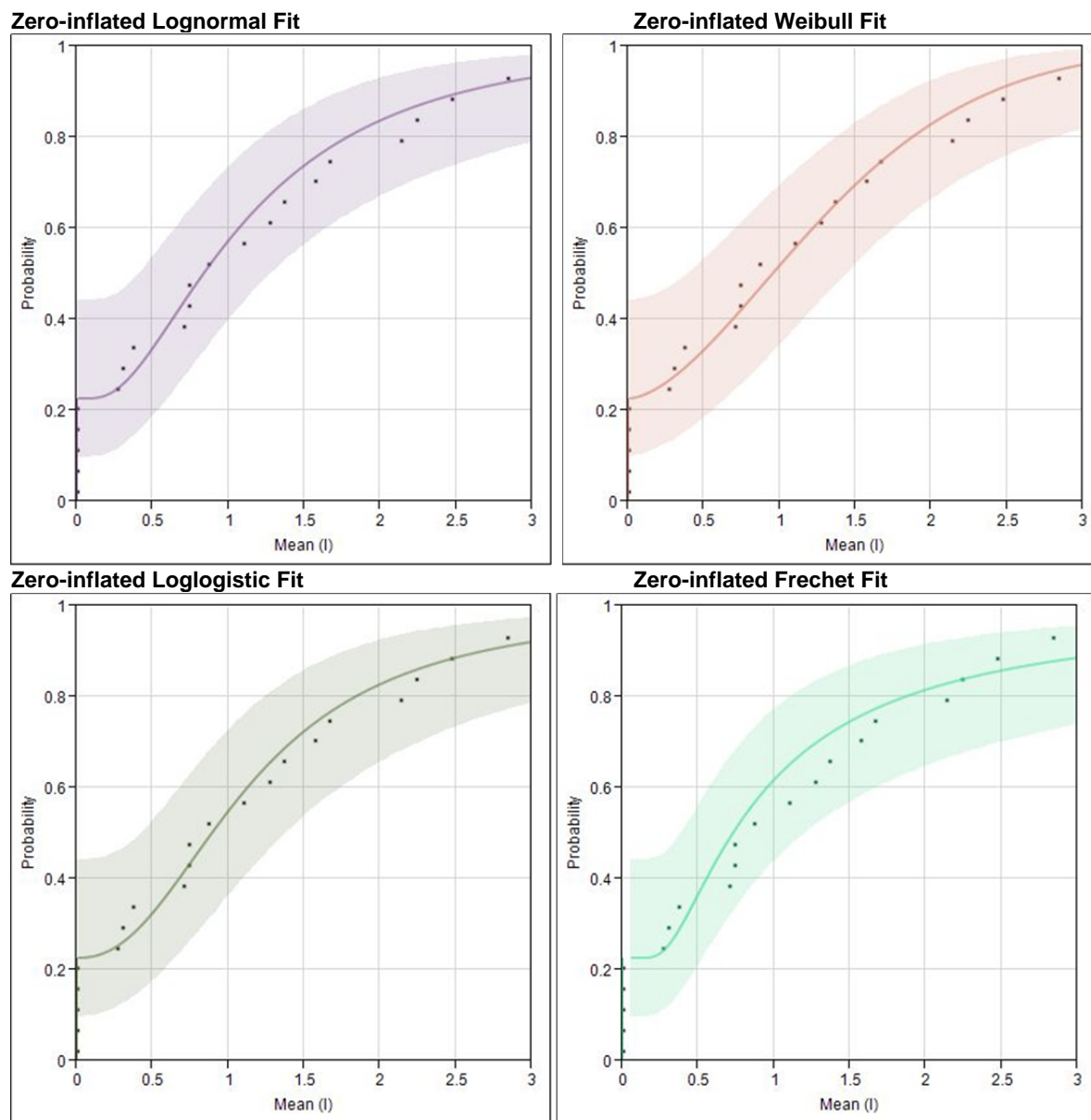


**Figure 3. Zero-inflated distribution models to the iodine saltstone  $K_d$  values: Lognormal, Weibull, Loglogistic, and Frechet. The "Zero-inflated" indicates that the negative  $K_d$  values were assigned zero values and treated uniquely in the distribution model.**

#### 4.4 EUROPIUM MEASURED IN CEMENTITIOUS MATERIALS

Precipitation of Eu precluded the ability to calculate  $K_d$  values. Eu concentrations were below detection limits for all samples in the no-solids controls and in the samples containing cementitious solids. Therefore the measured decreases in aqueous radionuclides were due to causes other than the sorption of the radionuclides by the added solid phases.

#### 4.5 EFFECT OF CEMENT CURE TEMPERATURE ON DISTRIBUTION COEFFICIENTS IN CEMENTITIOUS MATERIALS

Analysis of samples that were heated to 60 °C during curing for a short period of time (days) immediately after mixing demonstrated a marked improvement in  $K_d$  for Cs and Sr over samples cured between room temperature and ~55 °C (Table 4). Cure temperatures at or above ~60 °C change the physical properties of saltstone and this phenomenon may contribute to mechanisms that encourage sorption or precipitation of elements, such as Cs and Sr over room-temperature cured samples.

Metastable hydrates exist in cementitious materials at 25 °C. As temperature is increased, substantial changes in cement chemistry can be observed in blended cement phases. Glasser et al. (1991) performed a temperature effects study with cements containing BFS and OPC or FA. Results indicate that significant changes in  $\text{Ca(OH)}_2$  were observed for samples that were cured at 56 and 72 °C versus room temperature. Regardless of cure temperature, little change in  $\text{Ca(OH)}_2$  was observed between 3 months and 1 year, indicating that reactions between BFS and  $\text{Ca(OH)}_2$  to produce C-S-H continued at a slow rate or had stopped.

Glasser et al. reported XRD patterns of cementitious material containing a mixture of BFS and OPC at room temperature indicated ettringite, monosulfate, and  $\text{Ca(OH)}_2$  as the predominant (and expected) hydration products. However, samples cured to at 56 or 72 °C, aside from having reduced  $\text{Ca(OH)}_2$  levels, were absent of (or had significantly reduced) monosulphate, yet had an ingrowth of hydrogarnet.

Changes in hydration products resulting from elevated cure temperatures may affect mechanisms that control retention of ions in saltstone materials. Further investigation of the phases formed in saltstone samples heated at or above 60 °C while curing may help explain and validate the variability of  $K_d$  values observed for this select group of samples.

Previous experiments with SRNL-prepared laboratory samples have shown that increase in cure temperature can effect physical properties such as heat of hydration, dynamic Young's modulus, porosity, compressive strength, and set time (Harbour 2009).

#### 4.6 PLUTONIUM DISTRIBUTION COEFFICIENTS MEASURED IN SOILS

The sediment Pu  $K_d$  data is included in this study because it is a potential risk driver for the SRS PAs, and there are presently no direct studies of Pu variability in SRS soils. Instead the distribution of Pu sediment  $K_d$  values was assumed to be similar to other cations, as presented by

Kaplan (2010). The sediments used in this portion of the study were selected by a number of criteria identified in the Materials and Methods section, including the origin of soil, Pu oxidation state, and contact time with sediment (Table 12). They were further broken down into three broad categories to simulate three general types of plume:

- a far-field plume: pH 4.6 to 7.0,
- a high pH plume: pH >7.0, and
- a plume moving through a pH 4.6 to pH 10.47 system.

Much of the Pu sorption data that is reported as  $K_d$  values, especially the high pH Pu(IV) sorption data, indicates that Pu in the system has precipitated, as the reports demonstrated with the formation of Pu(IV) phases. Also, cement leachate is expected to be greater than pH 10.47, the largest pH value for which sorption experimental data was found. Higher pH data is necessary to confirm how soils will behave between 10.5 and pH 12. The properties of the sediments described in Table 12 are presented in Table 13.



**Table 12.** Pu  $K_d$  values selected from the literature used to develop the Pu  $K_d$  sediment distribution (sorted by pH).

Soil	pH	$K_d$ (mL/g)	Contact time (day)	source	Spike Pu Oxidation State
surface clay	4.63	3000	1	WSRC-TR-2003-00035; page 48	4
surface clay	4.67	13000	33	WSRC-TR-2003-00035; page 48	5
Subsurface Sand	4.69	110	33	WSRC-TR-2003-00035; page 46	5
Subsurface Sand	4.72	130	33	WSRC-TR-2003-00035; page 46	5
surface sand	4.78	1200	33	WSRC-TR-2003-00035; page 50	5
Subsurface Clay	4.81	2100	1	WSRC-TR-2003-00035; page 47	4
surface sand	4.82	510	6	WSRC-TR-2003-00035; page 49	5
Subsurface Sand	4.87	100	33	WSRC-TR-2003-00035; page 46	5
Subsurface Clay	4.95	9300	33	WSRC-TR-2003-00035; page 47	5
Subsurface Sand	5.10	600	33	WSRC-TR-2003-00035; page 46	5
Subsurface Sand	5.21	4800	33	WSRC-TR-2003-00035; page 46	5
Subsurface Sand	5.23	3700	33	WSRC-TR-2003-00035; page 46	5
surface sand	5.26	2900	6	WSRC-TR-2003-00035; page 49	5
Subsurface Clay	5.32	10000	33	WSRC-TR-2003-00035; page 47	5
Subsurface Sand	5.41	4900	33	WSRC-TR-2003-00035; page 46	5
Subsurface Sand	5.62	3100	33	WSRC-TR-2003-00035; page 46	5
surface clay	5.67	13000	33	WSRC-TR-2003-00035; page 48	5
Subsurface Clay	5.68	4700	33	WSRC-TR-2003-00035; page 47	5
Subsurface Clay	5.82	6600	1	WSRC-TR-2003-00035; page 47	4
surface sand	5.83	1400	6	WSRC-TR-2003-00035; page 49	5
Subsurface Sand	5.85	390	1	WSRC-TR-2003-00035; page 46	4
Subsurface Clay	5.98	9000	1	WSRC-TR-2003-00035; page 47	4
surface clay	6.02	4600	1	WSRC-TR-2003-00035; page 48	4
surface clay	6.05	13000	33	WSRC-TR-2003-00035; page 48	5
surface clay	6.09	1000	1	WSRC-TR-2003-00035; page 48	4
Subsurface Sand	6.10	2800	1	WSRC-TR-2003-00035; page 46	4
surface sand	6.13	1800	6	WSRC-TR-2003-00035; page 49	5
surface sand	6.34	1700	6	WSRC-TR-2003-00035; page 49	5
surface clay	6.55	8200	33	WSRC-TR-2003-00035; page 48	5
surface sand	6.56	400	6	WSRC-TR-2003-00035; page 49	5
Subsurface Sand	6.61	2500	1	WSRC-TR-2003-00035; page 46	4
surface sand	6.61	8300	33	WSRC-TR-2003-00035; page 50	5
Subsurface Clay	6.68	18000	1	WSRC-TR-2003-00035; page 47	4
surface sand	6.73	130	1	WSRC-TR-2003-00035; page 49	4
surface clay	6.81	33000	33	WSRC-TR-2003-00035; page 48	5
surface clay	6.83	3700	1	WSRC-TR-2003-00035; page 48	4
surface sand	6.89	8300	33	WSRC-TR-2003-00035; page 50	5
surface sand	6.98	270	6	WSRC-TR-2003-00035; page 49	5
surface sand	7.00	5700	33	WSRC-TR-2003-00035; page 50	5
Surface Sand	7.00	20000	33	WSRC-TR-2003-00035; page 50	5
Surface Clay	7.11	3500	1	WSRC-TR-2003-00035; page 48	4
Subsurface Clay	7.16	1600	33	WSRC-TR-2003-00035; page 47	5
Surface Clay	7.22	8200	33	WSRC-TR-2003-00035; page 48	5

Soil	pH	K <sub>d</sub> (mL/g)	Contact time (day)	source	Spike Pu Oxidation State
Subsurface Clay	7.32	3700	33	WSRC-TR-2003-00035; page 47	5
Surface Clay	7.36	33000	33	WSRC-TR-2003-00035; page 48	5
Surface Sand	7.36	20000	33	WSRC-TR-2003-00035; page 50	5
Surface Sand	7.36	20000	33	WSRC-TR-2003-00035; page 50	5
Surface Clay	7.49	33000	33	WSRC-TR-2003-00035; page 48	5
Surface Clay	7.53	13000	33	WSRC-TR-2003-00035; page 48	5
Surface Sand	7.58	20000	33	WSRC-TR-2003-00035; page 50	5
Subsurface Clay	7.69	1300	33	WSRC-TR-2003-00035; page 47	5
Subsurface Sand	7.70	2800	1	WSRC-TR-2003-00035; page 46	4
Subsurface Clay	7.74	600	33	WSRC-TR-2003-00035; page 47	5
Subsurface Clay	7.79	42000	1	WSRC-TR-2003-00035; page 47	4
Surface Sand	7.86	20000	33	WSRC-TR-2003-00035; page 50	5
Subsurface Clay	7.91	50000	1	WSRC-TR-2003-00035; page 47	4
Surface Sand	8.26	210	6	WSRC-TR-2003-00035; page 49	5
Subsurface Sand	8.42	20000	1	WSRC-TR-2003-00035; page 46	4
Surface Clay	8.49	1300	1	WSRC-TR-2003-00035; page 48	4
Subsurface Clay	8.89	540	33	WSRC-TR-2003-00035; page 47	5
Surface Clay	9.15	3300	33	WSRC-TR-2003-00035; page 48	5
Subsurface Sand	9.28	9300	1	WSRC-TR-2003-00035; page 46	4
Surface Clay	9.95	800	1	WSRC-TR-2003-00035; page 48	4
Surface Sand	10.47	290	1	WSRC-TR-2003-00035; page 49	4

<sup>a</sup> An SRS Pu K<sub>d</sub> data set that was purposely not included here was that of Prout (1958). The reason was because the SRS sediments were not characterized, experimental protocol was not specified in sufficient detail, and contact time was only one day,

Table 13. Characterization of sediments used in Pu  $K_d$  measurements discussed in Table 12.

Soil	Subsurface Clay	Subsurface Sand	Surface Clay	Surface Sand
% sand ( $>53 \mu\text{m}$ )	57.9	97	68	92
% silt ( $53 - 2 \mu\text{m}$ )	40.6	2.9	24	7
% clay ( $<2 \mu\text{m}$ )	1.6	0.2	8	1
Textural classification	Silty clay	Sand		
pH <sup>a</sup>	4.55	5.1	5.8	4.7
% OM <sup>b</sup>	1.21	0.35	3.2	0.8
CEC (cmol/kg) <sup>c</sup>	$1.09 \pm 0.31$	$-0.35 \pm 0.22$		
AEC (cmol/kg) <sup>c</sup>	$1.58 \pm 0.61$	$0.06 \pm 0.19$		
BET surface area ( $\text{m}^2/\text{g}$ )	15.31	1.27	9.2	1.4
Single point surface area ( $\text{m}^2/\text{g}$ )	15.07	1.24		
CDB extractable Fe ( $\text{mg/g}$ ) <sup>c</sup>	15.26	7.06		
Al (ppm)	63.59	16.64		
Na (ppm)	42.91	34.69		
Mg (ppm)	144.05	98.76		
Ca (ppm)	64.41	24.62		
K (ppm)	182.87	92.97		
Mineralogy (based on XRD)	Kao > goeth > Hem (no qtz or 14 A)	Kao > goeth > musco/14A (no qtz)	Kao > chlorite/verm . qtz > goeth > gibb > rutile	Chlorite/vermiculite > quartz > kaolinite > illite
<sup>a</sup> pH procedure from Chemical Analysis of Ecological Materials, Stewart E. Allen, pgs. 16-17. <sup>b</sup> OM procedure from Chemical Analysis of Ecological Materials, Stewart E. Allen, pgs. 15-16. <sup>c</sup> CDB procedure from Methods of Soil Analysis Part 3-Chemical Methods, D.L. Sparks pgs 1228-1220. <sup>d</sup> Ion extraction procedure from Methods of Soil Analysis Part 3-Chemical Methods, D.L. Sparks pgs 1218-1220; 0.2 M $\text{NH}_4\text{Cl}$ . <sup>e</sup> CEC/AEC procedure from Methods of Soil Analysis Part 3-Chemical Methods, D.L. Sparks pgs 1218-1220; Unbuffered Salt Extraction Method.				

#### 4.6.1 Entire Pu $K_d$ Data Set: All pH Values

The Pu  $K_d$  values ranged from 107 to 50,000 and the mean was  $8559 \pm 11,241$  mL/g (Table 14). This is not an unexpected standard deviation considering the wide range of conditions that the  $K_d$  values were measured under and the wide variety of Pu species that exist in SRS sediments between pH 4.6 and 11 (unlike the almost uniform speciation of  $\text{Cs}^+$  in groundwater). The coefficient of variance (CV) or percent standard deviation is over 100% and there is positive skewness, so the data is far from normal or symmetrical.

This large range of Pu  $K_d$  values is not uncommon under natural environmental conditions due to the wide range of parameters that influence Pu sorption to sediments (e.g., oxidation state, pH, natural organic matter, mineralogy, microbial populations, Eh, Fe-oxide coatings). There are three estimates of Pu  $K_d$  values ranges in nature, albeit, not under SRS site specific conditions:

- Thibault et al. (1990) reported a range in sandy soils of 27 to 36,000 mL/g with a geometric mean of 550 mL/g based on a literature review
- Baes and Sharp (1983) reported a range in agricultural soils of 11 to 300,000 mL/g in agricultural soils with a mean of geometric mean of 1800 mL/g, based on a literature review and thermodynamic calculations.
- Coughtrey et al. (1985) reported a range of Pu  $K_d$  in all sediments 18 to 10,000 mL/g with a best estimate of 5000 mL/g.

The range of 100 to 50,000 and a median of 3,700 is consistent with those previously reported. The smaller range can be attributed to the fact that only sediments from one location, the SRS, were included in this distribution.

Table 14. Quantiles and descriptive statistics of the full data set of Pu  $K_d$  values.

<b>Quantiles and Descriptive Statistics for <math>K_d</math></b>		
100.0%	maximum	50,000
99.5%		50,000
97.5%		44,800
90.0%		20,000
75.0%	quartile	13,000
50.0%	median	3,700
25.0%	quartile	1,250
10.0%		282
2.5%		106.5
0.5%		100
0.0%	minimum	100
<b>Descriptive Statistics</b>		
Mean		8559.6923
Std Dev		10823.635
Std Err Mean		1342.5067
Upper 95% Mean		11241.658
Lower 95% Mean		5877.7268
N		65
Variance		117151081
Skewness		1.9212208
Kurtosis		3.7264401
CV		126.44888
N Missing		0

Table 15 provides the goodness-of-fit for the full data set of the Pu  $K_d$  values. It is a rank ordering from best to worst. Three global metrics for a good fit were used. The Weibull model had the best overall fit on two of three measures, since it has lower values for those metrics.

**Table 15. Goodness-of-fit of distribution models for full data set of  $K_d$  values in soil.**

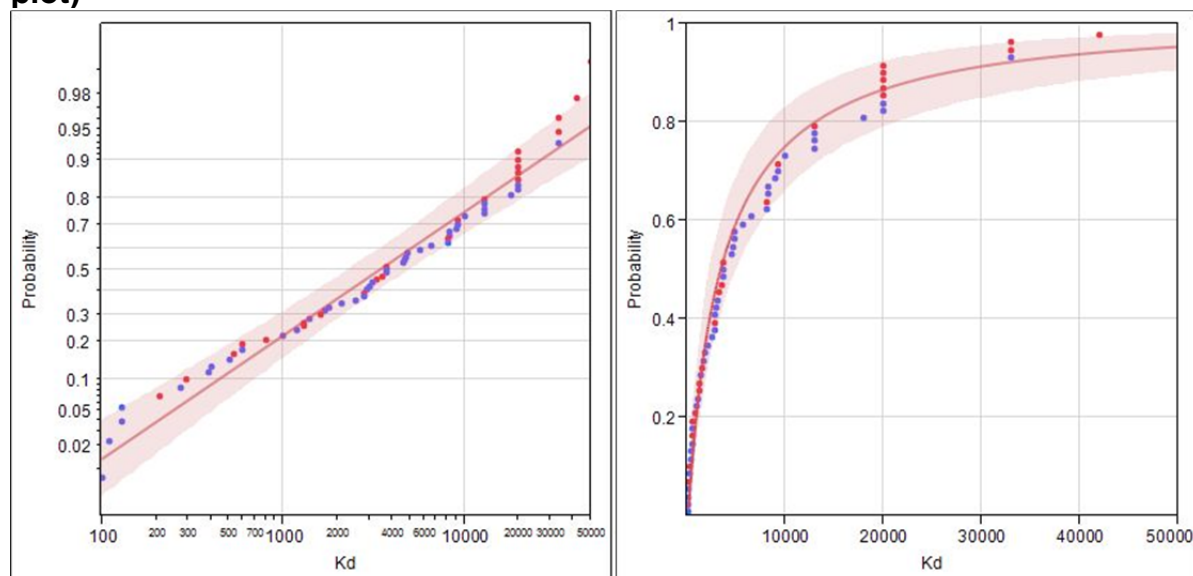
<b>Distribution</b>	<b>AICc</b>	<b>-2Loglikelihood</b>	<b>BIC</b>
Weibull	1,301	1,296.8	1,305
Generalized Gamma	1,303	1,296.6	1,309
Lognormal	1,305	1,300.6	1,309
Loglogistic	1,308	1,303.7	1,312
Exponential	1,309	1,307.1	1,311
Log Generalized Gamma	1,314	1,307.8	1,320
Frechet	1,320	1,315.5	1,324
LEV	1,358	1,353.7	1,362
Logistic	1,384	1,380.3	1,389
Normal	1,395	1,391.1	1,399
SEV	1,436	1,432.1	1,440

<sup>a</sup> AIC: Akaike information criterion; BIC: Schwartz's Bayesian information criterion; -2 log likelihood: -2 times the natural log of the likelihood evaluated with the best-fit estimates of the parameters

A good fit is shown by the data points coming close to the straight line on the left of Figure 4.

Statistics give you a “global” view of what is a good fit. These plots show where the fit may be weak. Then it is up to the scientist together with the statisticians to decide whether it is a good fit. For example, the performance assessment may be more sensitive to low  $K_d$  values than high  $K_d$  values, and for this reason, we may select a model that is more accurate at fitting low  $K_d$  values than at fitting global  $K_d$  values identified by global goodness-of-fit parameters. Weibull appears to be the better fit, with possibly the exception of the lowest  $K_d$  value. As will be shown below, the Weibull distribution will also be a reasonable fit for the pH 4.6 to 7 data set and for the pH >7.0 data set.

**Lognormal Fits: Left (quantile plot: log scale on x-axis)) and Right (nonparametric plot)**



**Weibull Fits: Left (quantile plot: log scale on x-axis) and Right (nonparametric plot)**

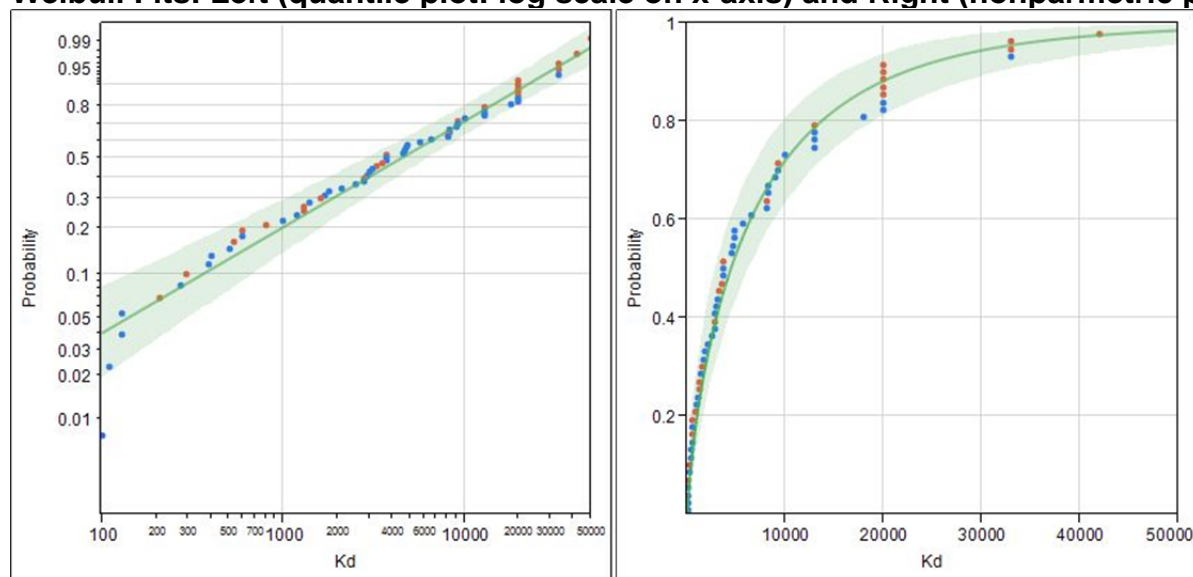


**Figure 4. Lognormal and Weibull distribution fits to the entire data set of sediment Pu  $K_d$  values. The red dots indicate  $\text{pH} > 7.0$  and blue dots indicate  $\text{pH} \leq 7$ . Shaded area is the 95% confidence region.**

#### 4.6.2 pH >7.0 Pu K<sub>d</sub> Data Set

The range of Pu K<sub>d</sub> values is 210 to 50,000 and the mean is  $12,851 \pm 14,525$  (Table 16). Again, the skewness and kurtosis suggests that the shape of the distribution is not symmetrical, although in this case the peak of the curve, it is not nearly as flat as some of the previous distributions (kurtosis). The coefficient of variance is quite high even though the pH range was greatly limited, suggesting that pH is not the only controlling factor of Pu K<sub>d</sub> values.

Table 16. Quantiles and descriptive statistics of the pH >7.0 Pu K<sub>d</sub> data set.

<b>Quantiles and Descriptive Statistics for K<sub>d</sub></b>		
100.0%	maximum	50,000
99.5%		50,000
97.5%		50,000
90.0%		37,500
75.0%	quartile	20,000
50.0%	median	5,950
25.0%	quartile	1,300
10.0%		415
2.5%		210
0.5%		210
0.0%	minimum	210
<b>Descriptive Statistics</b>		
Mean		12851.667
Std Dev		14525.527
Std Err Mean		2965.0109
Upper 95% Mean		18985.259
Lower 95% Mean		6718.0744
N		24
Variance		210990945
Skewness		1.1859828
Kurtosis		0.5875395
CV		113.02446
N Missing		0

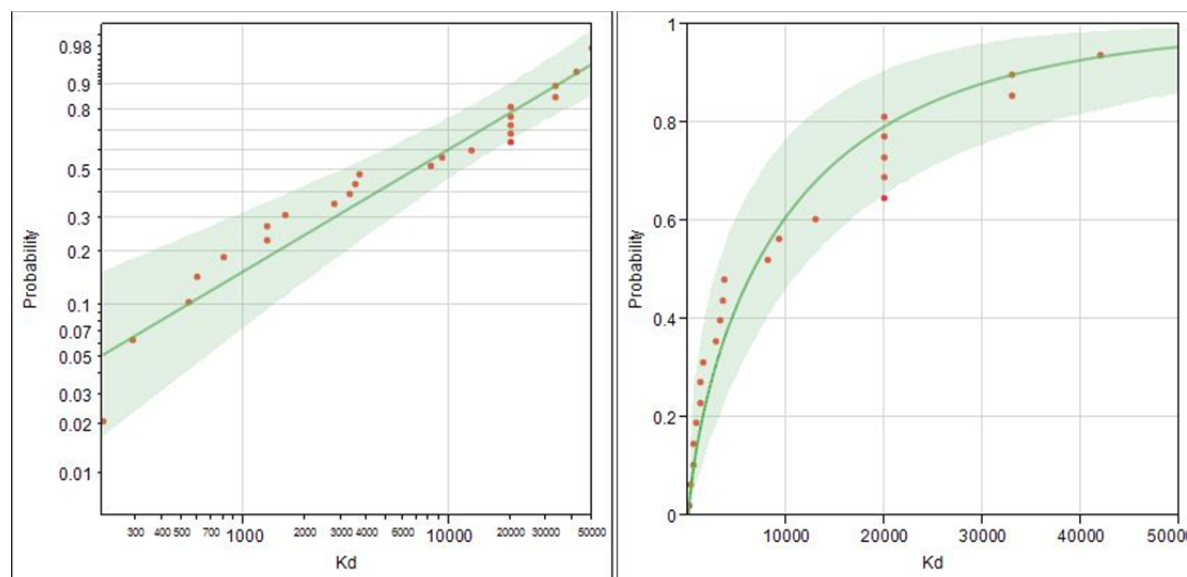


Table 17 provides a goodness-of-fit for the pH>7.0 Pu  $K_d$  data set: lower the value, the better the distribution model fit to the data. The table provides a listing from best to worst. Three global metrics for good fit were used. The Weibull model had the best overall fit on all three measures.

**Table 17. Goodness-of-fit of distribution models for the pH >7.0 Pu  $K_d$  data set.**

Distribution	AICc	-2Loglikelihood	BIC
Weibull	502.92655	498.35512	504.71123
Exponential	504.32080	502.13898	505.31704
Lognormal	504.36121	499.78978	506.14589
Generalized Gamma	504.70366	497.50366	507.03782
Threshold Lognormal	505.99122	498.79122	508.32538
Loglogistic	506.50000	501.92857	508.28468
Frechet	508.29970	503.72828	510.08438
Log Generalized Gamma	509.40925	502.20925	511.74342
LEV	523.47072	518.89929	525.25540
Logistic	531.49327	526.92184	533.27794
Normal	531.67487	527.10344	533.45955

<sup>a</sup> AIC: Akaike information criterion; BIC: Schwartz's Bayesian information criterion; -2 log likelihood: -2 times the natural log of the likelihood evaluated with the best-fit estimates of the parameters



**Figure 5. Weibull fits to the quantile plot (left) and nonparametric plot (right).**

### 4.6.3 Pu $K_d$ Data Set for $\text{pH} \leq 7.0$

The sediment Pu  $K_d$  data ranged from 100 to 33,000 mL/g when the pH was restricted to 4.6 to 7.0 or less, simulating far-field conditions, the conditions far from the chemical influence from the source term (Table 18). The mean Pu  $K_d$  was  $6047 \pm 6971$  mL/g (Table 18). Again, the standard deviation is extremely large, as was the case with the entire data set indicating that limiting the pH does not reduce variance. The kurtosis is especially high, indicating the data is spread out.

Table 18. Quantiles and descriptive statistics of the  $\text{pH} \leq 7.0$  Pu  $K_d$  data set.

<b>Quantiles and Descriptive Statistics for <math>K_d</math></b>		
100.0%	maximum	33,000
99.5%		33,000
97.5%		32,350
90.0%		17,000
75.0%	quartile	8,650
50.0%	median	3,700
25.0%	quartile	1,100
10.0%		158
2.5%		100.5
0.5%		100
0.0%	minimum	100
<b>Descriptive Statistics</b>		
Mean		6047.3171
Std Dev		6971.3327
Std Err Mean		1088.7393
Upper 95% Mean		8247.7412
Lower 95% Mean		3,846.893
N		41
Variance		48599480
Skewness		1.9704897
Kurtosis		4.688515
CV		115.27976
N Missing		0

Table 19 provides a goodness-of-fit for the  $\text{pH} \leq 7.0$  Pu  $K_d$  data set: lower the goodness-of-fit value, the better the model fit. The table provides a listing from best to worst. Three global metrics for good fit were used. The top three distributions each are best on one of three global goodness-of-fit metrics. The Weibull, Generalized Gamma, Loglogistic, and Lognormal have been commonly among the better models.

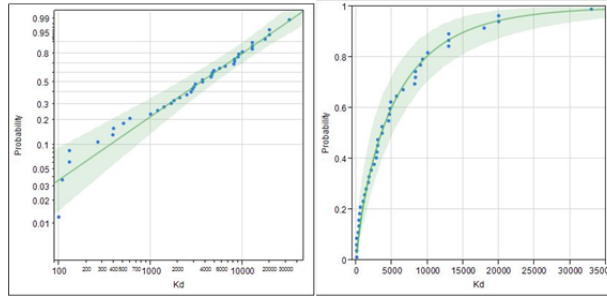
**Table 19. Goodness-of-fit of distribution models for the Pu  $K_d$  data set for  $\leq \text{pH } 7.0$ .**

<b>Distribution</b>	<b>AICc</b>	<b>-2Loglikelihood</b>	<b>BIC</b>
Weibull	797.51453	793.19874	800.62588
Exponential	798.10690	796.00434	799.71791
Generalized Gamma	799.75680	793.10815	804.24887
Lognormal	802.73341	798.41762	805.84477
Log Generalized Gamma	802.82501	796.17636	807.31708
Loglogistic	804.00174	799.68595	807.11309
Frechet	814.22946	809.91367	817.34081
LEV	823.67835	819.36256	826.78970
Logistic	838.55733	834.24154	841.66868
Normal	845.32041	841.00462	848.43177
SEV	872.39809	868.08231	875.50945

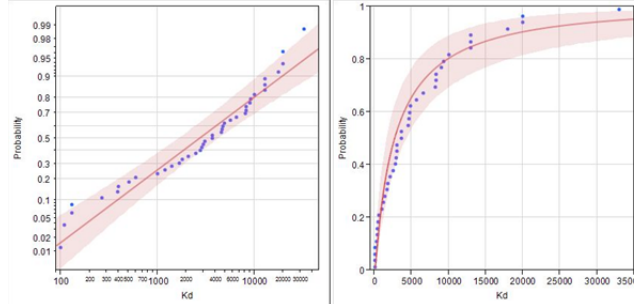
<sup>a</sup> AIC: Akaike information criterion; BIC: Schwartz's Bayesian information criterion; -2 log likelihood: -2 times the natural log of the likelihood evaluated with the best-fit estimates of the parameters

The distribution model fits for the sediment Pu  $K_d$  data of  $\text{pH} \leq 7.0$  are presented in Figure 6. The lognormal clearly does not fit as well as the Weibull model, with many of the lower and mid-range  $K_d$  values not falling on the lines (Figure 6). The extended generalized gamma models the data well, however, as noted earlier, it is a more complicated model, requiring additional fitting parameters. In fact, it is a special case of the Weibull model. With the extra fitting parameter the extended generalized gamma model does an excellent job of fitting the data.

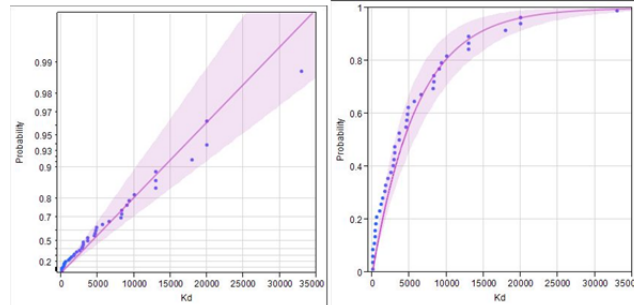
**Weibull Fits: Left (quantile plot: log scale on x-axis) and Right (nonparametric plot)**



**Lognormal Fits: Left (quantile plot: log scale on x-axis) and Right (nonparametric plot)**



**Exponential Fits: Left (quantile plot: log scale on x-axis) and Right (nonparametric plot)**



**Extended Generalized Gamma Fits: Left (quantile plot: log scale on x-axis) and Right (nonparametric plot)**

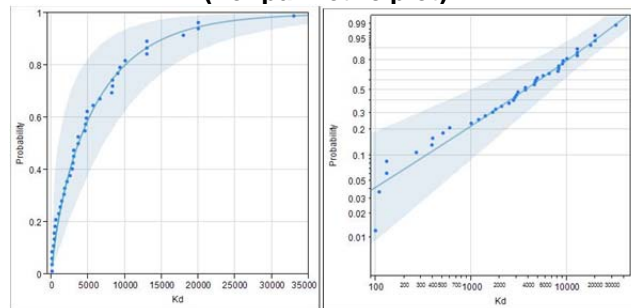


**Figure 6. Weibull, lognormal Exponential and Extended Generalized Gamma model fits to the Pu  $K_d$  data of  $\text{pH} \leq 7$ .**

#### 4.6.4 Subsets of the Pu $K_d$ Data Set based on pH and Sediment Texture

Additional statistical analyses were conducted with just the sandy sediments ( $n = 33$ ) and just the clayey sediments ( $n = 31$ ) for  $pH > 7$  and  $\leq 7$ . Distribution quantile plots were drawn, AIC, -2loglikelihood, and BIC model fits were conducted to the dozen or so distribution models (Weibull, lognormal, Frechet, normal, etc.). Generally, the results are presented in Appendix A and Table 20. The Pu  $K_d$  ranges did not decrease greatly by categorizing the  $K_d$  by sediment type and pH (e.g., Clay/ $\leq pH 7$ , Clay  $> pH 7$ , etc...) and perhaps equally important is that the types of distribution models did not change greatly either. For this reason, statistics based on all soil types, the most robust data set, were used to develop the recommended model input parameters.

The mean Pu  $K_d$  value in each of these categories ranged from 3,830 mL/g (Sandy sediment/ $pH \leq 7$ ) to 13,058 mL/g (Clayey sediment/ $pH > 7$ ), and as such may represent the best estimate for a  $K_d$  value for these conditions (Table 20).

**Table 20.** Quantile and statistical analysis of sediment Pu  $K_d$  values in entire data set, sandy sediment, and clayey sediments.

		All soil	All soil	All Soil	Sand	Sand	Clay	Clay
		All pH	pH>7.0	pH≤7.0	pH >7.0	pH ≤7.0	pH >7.0	pH ≤7.0
100.0%	Max	50,000	50,000	33,000	20,000	20,000	50,000	33,000
99.5%		50,000	50,000	33,000	20,000	20,000	50,000	33,000
97.5%		44,800	50,000	32,350	20,000	20,000	50,000	33,000
90.0%		20,000	37,500	17,000	20,000	12,980	45,200	22,500
75.0%	quartile	13,000	20,000	8,650	20,000	4,850	33,000	13,000
50.0%	median	3,700	5,950	3,700	20,000	1,800	3,500	8,600
25.0%	quartile	1,250	1,300	1,100	1,545	395	1,300	3,925
10.0%		282	415	158	210	122	576	1,770
2.5%		106.5	210	100.5	210	100	540	1,000
0.5%		100	210	100	210	100	540	1,000
0.0%	Min	100	210	100	210	100	540	1,000
<b>Statistic</b>								
Mean		8560	12852	6047	12511	3830	13056	9513
Std Dev		10824	14526	6971	9258	5428	17249	7839
Std Err Mean		1343	2965	1089	3086	1086	4454	1960
Upper 95% Mean		11242	18985	8248	19628	6070	22608	13690
Lower 95% Mean		5878	6718	3847	5395	1589	3504	5335
N		65	24	41	9	25	15	16

#### 4.6.5 Input Weibull Distribution Values

Table 21 and Table 22 contain input values for Weibull distributions for soil Pu  $K_d$  values and zero-inflated Weibull distributions for cement iodine  $K_d$  values. These values are for young and middle aged, oxidized cementitious materials.

**Table 21.** Parametric Estimate for GoldSim Calculated from Statistical Modeling of Weibull Distributions for Pu  $K_d$  Values.

Distribution	Minimum <sup>a</sup>	Weibull Slope	Mean-Minimum
Sand/all pH	100	0.555	6702
Sand/pH >7	210	0.499	18,234
Sand/pH ≤7	100	0.560	4,096
Clay/all pH	540	0.696	11,021
Clay/pH ≤7 <sup>b</sup>	0	1.000	9,512
Clay/pH >7	540	0.485	14,620

<sup>a</sup> Minimum is the statistically the best fitted value.  
<sup>b</sup> The distribution for the Clay/pH ≤7 was also very well described as an exponential distribution with alpha (the mean) equal to 9,512. Either distribution is equally good for describing Pu  $K_d$  values under these pH conditions.

**Table 22.** Input GoldSim Parametric Estimates for the Zero-Inflated Weibull Distributions for Cement Iodine  $K_d$  Values.

Distribution	Probability $K_d = \text{zero}$	Probability $K_d = \text{Weibull distribution}$	Minimum	Weibull Slope	Mean-minimum
Iodine in cement	0.25	0.75	0.0	1.377	1.596

Zero-inflated Weibull can be implemented in GoldSim by using the Discrete Distribution model to first separate whether the  $K_d$  is part of the 0 mL/g population or part of the non-zero Weibull population. An if/then statement can be used to send the non-zero data to a Weibull distribution.

#### 4.6.6 Recommended Values for Performance Assessments

Based on the recommendation in Kaplan (2010), the **best estimate** for a Pu  $K_d$  value in sandy sediments was 290 mL/g and in clayey sediments was 5950 mL/g. Using the pH ≤7 data, the 290 mL/g sand  $K_d$  value would fall between the 10-25 percentile range (Table 20). Similarly, the 5950 mL/g clay  $K_d$  value would fall in the 25-50 percentile quantile.

Recently, and not reflected in the data set presented in Table 12, was a series of studies conducted in lysimeters on the SRS (Demirkanli et al., 2008, 2009; Demirkanli et al., 2007; Kaplan et al., 2006; Kaplan et al., 2010; Kaplan et al., 2007). These experiments reflect a higher-pedigree measurement of how Pu would behave under SRS conditions than in a short-term laboratory batch setting. In this field experiment, which lasted 11 years, Pu of varying

oxidation state (Pu(III), Pu(IV), and Pu(VI)), moved very little when exposed to natural rainfall conditions; the Pu moved through the sediment at an overall rate of <4cm/11 yr. A kinetic and solubility model (the model used 4 input values to describe Pu geochemistry, instead of a single Pu  $K_d$  value) was used to describe transport through these field lysimeters, but the single best  $K_d$  value was ~1800 mL/g ((Demirkanli et al., 2009). To date this is our best experimental estimate of a single sediment Pu(IV)  $K_d$  value. However, this lysimeter sediment contained more clay-size particles, than what is typically consider a “sandy sediment” on the SRS, thus biasing the  $K_d$  higher than expected for a sandy sediment.

It is suggested that the best-estimate for Pu  $K_d$  values in sandy sediment be increased from 290 to 650 mL/g because: 1) recent lysimeter data indicate that the experimental best estimate  $K_d$  value is in fact much closer to 1800 mL/g, and 2) quantile data indicate that the 290 mL/g data is in the lower quantiles and while conservative, may not represent a best-estimate.

Presently, there is only an empirical approach in the PA to alter  $K_d$  values to account for the impact of cementitious leachate chemistry; it is through the “cementitious leachate impact factor” (Table 2 in Kaplan 2010). This multiplier or factor can either increase  $K_d$  values, as is the case for Pu (x2) and Sr (x3), or decrease  $K_d$  values, as is the case with I (x0.1)  $K_d$  values, or have no impact on  $K_d$  values, as is the case for Cs (x1). The influence depends on chemical considerations. In the case of Pu, the presence of the cementitious leachate promotes precipitation, whereas with iodine, it promotes anion ( $\text{OH}^-$ ) competition. The cementitious leachate impact factor for Pu is “2” and for I, it is “0.1.”

Prikyrl and Pickett (2007) recommended a Pu  $K_d$  value for aquifer sediment  $K_d$  of 250 mL/g. Their recommendation was based on similar data as presented in Kaplan (2006; 2010), which had recommended best estimate Pu  $K_d$  values of 290 mL/g. The Pu  $K_d$  dataset in Table 12 includes all the Pu  $K_d$  data considered by Prikyrl and Pickett (2007) except this report did not include data from Prout (1958) because he used a Pu-soil contact time of only 1 day and used distilled water (which is too unlike groundwater), and did not use the data from Hoeffner (1985) because the oxidation state of the Pu was not verified.

The recommended input for the Weibull distribution for the Pu  $K_d$  values are presented in Table 23, those for the Zero-inflated Weibull distribution for cement iodine  $K_d$  values are presented in Table 22.

**Table 23.** Recommended Parametric Estimate for Weibull Distributions for Pu  $K_d$  Values

Distribution	Minimum <sup>a</sup>	Weibull Slope	Mean-Minimum
Sand/pH≤7	100	0.56	650
Clay/pH ≤7	100	0.56	5950

## 5.0 CONCLUSIONS

This report contains results from two tasks. The first task measured Cs, Sr, I, and Eu  $K_d$  values with simulated saltstone. The second task consisted of a critical literature review and statistical analysis of soil Pu  $K_d$  values. For both tasks the statistical range and distribution were determined to assist stochastic modelers in site wide PA analyses.

*Saltstone  $K_d$  Task* – The objective of the saltstone  $K_d$  variability project was to determine the range and distribution of cesium, strontium, iodine and europium  $K_d$  values in saltstone. The scope of this study did not include understanding saltstone sorption mechanisms responsible for increasing or decreasing sorption. Cs, Sr, and I  $K_d$  values were measured from a wide range of formulations of 22 archived saltstone materials (measured in triplicate). Eu  $K_d$  values could not be measured because Eu precipitated or sorbed to glassware during the experiment. The following  $K_d$  ranges, means, and standard deviations were obtained:

- saltstone triplicate Cs  $K_d$  values ranged from 5 to 436 mL/g (mean  $K_d = 20 \pm 15$  mL/g for <60 °C samples; mean  $K_d = 289 \pm 115$  mL/g for 60 °C samples),
- saltstone triplicate Sr  $K_d$  values ranged from 122 to 6,938 mL/g (mean  $K_d = 528 \pm 242$  mL/g for <60 °C samples; mean  $K_d = 3383 \pm 2401$  mL/g for 60 °C samples)
- saltstone triplicate I  $K_d$  values ranged from -1.5 to 2.9 mL/g (mean  $K_d = 1.07 \pm 0.97$  mL/g for all samples)

The distribution of saltstone  $K_d$  values were very wide, capturing the wide array of formulations and temperature curing conditions represented in the samples.

This work suggests keeping the present method of calculating  $K_d$  value ranges for stochastic models:

$$\begin{aligned}\text{“Min”} &= K_d - (1.5 * 0.5 * K_d) = 0.25 * K_d \\ \text{“Max”} &= K_d + (1.5 * 0.5 * K_d) = 1.75 * K_d\end{aligned}$$

This range is not as large as identified experimentally. It is possible that the experimental conditions selected are not in fact those that may prevail in the field. Furthermore, only a small number of samples were analyzed. Two types of distributions were selected for the cementitious materials. Lognormal is used for the cations (Cs, Sr etc...) and the zero-inflated Weibull for the anions that used  $K_d$  values including  $K_d = 0$  (e.g. I). The Weibull and lognormal are very common distributions that are available in the GoldSim software presently used on the SRS for stochastic modeling for various PAs.

An unrelated and unexpected result from this research was that Cs and Sr  $K_d$  values were consistently much greater than expected, especially when the samples were cured at a temperature of at least 60 °C. This study was not designed to evaluate temperature effects on sorption and as such more research is necessary to confirm these findings. Regarding this latter



finding, more research is needed to validate this observation and understand the mechanism as knowledge on how curing profiles affect  $K_d$  is relevant to the PA and could lead to saltstone formulations that have improved performance properties. It is possible that Cs and Sr  $K_d$  variance could be greatly reduced through accounting for temperature. Stated differently, it may be necessary to measure saltstone  $K_d$  values with materials that have been temperature cured in a manner similar as the Saltstone Facility.

*Soil Pu  $K_d$  Task* – The range and distribution of plutonium  $K_d$  values in soils is not known. 65 SRS sediment Pu- $K_d$  values were critically reviewed, tabulated, and then statistically analyzed to identify their range and distributions, similar to what was done with the saltstone  $K_d$  values. Further refinement of the distributions was made based on the soil texture and soil pH range. The purpose of the Pu sediment  $K_d$  dataset was not to attempt to understand through statistics how to better understand Pu sorption to sediments or to lower Pu  $K_d$  variance. The following  $K_d$  ranges, means, and standard deviations were obtained:

- pH 4.6 to 10.47 sediment Pu  $K_d$  values ranged from 100 to 50,000 mL/g (mean  $K_d$  =  $8,559 \pm 10,823$  mL/g; to simulate a plume moving through all pH conditions),
- pH 4.6 to 7.0 sediment Pu  $K_d$  values ranged from 100-33,000 mL/g (mean =  $6,047 \pm 6,971$  mL/g ; to simulate a plume moving through far-field conditions),
- pH 7.01 to 10.47 sediment Pu  $K_d$  values ranged from 210 – 50,000 mL/g (mean =  $12,851 \pm 14,525$  mL/g; to simulate a plume moving through a basic cementitious plume conditions), and

The Weibull distribution was recommended for each of the Pu sediment distributions. The large range in Pu  $K_d$  was a result of a sharp rise or drop in  $K_d$  values, consequently, if the intent is to reduce the range of  $K_d$  values, then smaller ranges of pH values are recommended. The recommended best estimate Pu  $K_d$  value for sandy sediments was increased from 290 to 650 mL/g based on long-term field lysimeter studies, and the observation that the 290 mL/g value was within the 10-25 percentile of Pu  $K_d$  values in sandy sediments.

## 6.0 REFERENCES

- Allard, B., L. Eliasson, S. Hoglund, and K. Andersson. 1984. Sorption of Cs, I and Actinides in Concrete Systems. SKB Technical Report SKB/KBS TR-84-15, SKB, Stockholm, Sweden.
- Almond, P. M., and D. I. Kaplan. 2011. Distribution Coefficients ( $K_d$ ) Generated from a Core Sample Collected from the Saltstone Disposal Facility. SRNL-STI-2010-00667.
- Atkins, M., and F. P. Glasser. 1992. Application of Portland Cement-Based Materials to Radioactive Waste Immobilization. *Waste Management*. 12:105–131.
- Baes, C. F., III, and R. D. Sharp. 1981. A proposal for Estimating of Soil Leaching Constants for Use in Assessment Models.. *Journal of Environmental Quality* 12:17-28.
- Claeskens, G, and N.L. Hjort. 2008. Model Selection and Model Averaging. Cambridge University Press. New York.
- Coughtrey, P.J., D. Jackson, and M. C. Thorne. 1985. Radionuclide Distribution and Transport in Terrestrial and Aquatic Ecosystems. A Compendium of Data. A. A. Balkema, Netherlands.
- Demirkanli, D. I., Molz, F. J., Kaplan, D. I., and Fjeld, R. A. (2008). A fully transient model for long-term plutonium transport in the Savannah River Site vadose zone: Root water uptake. *Vadose Zone Journal* 7, 1099-1109.
- Demirkanli, D. I., Molz, F. J., Kaplan, D. I., and Fjeld, R. A. (2009). Soil-Root Interactions Controlling Upward Plutonium Transport in Variably Saturated Soils. *Vadose Zone Journal* 8, 574-585.
- Demirkanli, D. I., Molz, F. J., Kaplan, D. I., Fjeld, R. A., and Coates, J. T. (2007). Modeling plutonium transport through sediment containing plutonium sources of various oxidation states: An 11-year lysimeter study. *Abstracts of Papers of the American Chemical Society* 233.
- Harbour, J. R., T. B. Edwards, E. K. Hansen, and V. J. Williams. 2007. Impact of Increased Aluminate Concentrations on Properties of Saltstone Mixes. WSRC-STI-2007-00506.
- Harbour, J. R., V. J. Williams. 2008. Saltstone performance Indicator – Dynamic Young’s Modulus. SRNL-STI-2008-00488.
- Harbour, J. R., T. B. Edwards, and V. J. Williams. 2009. Impact of Time/Temperature Curing Conditions and Aluminate Concentration on Saltstone Properties. SRNL-STI-2009-00184.

- Hoeffner, S.L. 1985. Radionuclide Sorption on Savannah River Plant Burial Ground Soil—A Summary and Interpretation of Laboratory Data. DP-1702. Aiken, South Carolina: E.I. du Pont de Nemours and Company, Savannah River Laboratory.
- Hoglund, S., L. Eliasson, B. Allard, K. Andersson, and B. Torstenfelt. 1985. Sorption of some Fission Products and Actinides in Concrete Systems. *Mat. Res. Soc. Symp. Proc.* 50:683-690.
- Kaplan, D. I., D. I. Demirkanli, L. Gumapas, B. A. Powell, R. A. Fjeld, F. J. Molz, S. M. Serkiz 2006. 11-Year Field Study of Pu Migration from Pu III, IV, and VI Sources. *Environmental Science and Technology*, 40(2): 443-448.
- Kaplan, D. I. and R. J. Serne. 1998. Pertechetate Exclusion from Sediments. *Radiochim. Acta.* 81: 117-124.
- Kaplan, D. I., and J. T. Coates. 2007. Partitioning of Dissolved Radionuclides to Concrete under Scenarios Appropriate for Tank Closure Performance Assessments. WSRC-TR-2007-00640, Rev. 0. Washington Savannah River Company, Aiken, SC 29808.
- Kaplan, D. I. (2010). "Geochemical Data Package for Performance Assessment Calculations Related to the Savannah River Site," Rep. No. SRNL-STI-2009-00473. Savannah River National Laboratory, Aiken, SC.
- Kaplan, D. I., D. I. Demirkanli, L. Gumapas, B. A. Powell, R. A. Fjeld, F. J. Molz, S. M. Serkiz (2006). 11-Year Field Study of Pu Migration from Pu III, IV, and VI Sources. *Environmental Science and Technology* 40, 443-448.
- Kaplan, D. I., Demirkanli, D. I., Gumapas, L., Powell, B. A., Fjeld, R. A., Molz, F. J., and Serkiz, S. M. (2006). Eleven-year field study of Pu migration from PuIII, IV, and VI sources. *Environmental Science & Technology* 40, 443-448.
- Kaplan, D. I., Demirkanli, D. I., Molz, F. J., Beals, D. M., Cadieux, J. R., and Halverson, J. E. (2010). Upward movement of plutonium to surface sediments during an 11-year field study. *Journal of Environmental Radioactivity* 101, 338-344.
- Kaplan, D. I., Powell, B. A., Demirkanli, D. I., Fjeld, R. A., Molz, F. J., Serkiz, S. M., and Coates, J. T. (2004). Influence of oxidation states on plutonium mobility during long-term transport through an unsaturated subsurface environment. *Environmental Science & Technology* 38, 5053-5058.
- Kaplan, D. I., Powell, B. A., Duff, M. C., Demirkanli, D. I., Denham, M., Fjeld, R. A., and Molz, F. J. (2007). Influence of sources on plutonium mobility and oxidation state transformations in vadose zone sediments. *Environmental Science & Technology* 41, 7417-7423.

- McDowell-Boyer, L. and D. I. Kaplan. 2009. *Distribution Coefficients ( $K_{ds}$ ), Distributions, and Cellulose Degradation Product Correction Factors for the Composite Analysis*, April, 2009, SRNL-STI-2009-00150, Savannah River National Laboratory, Aiken, SC.
- Powell, B. A., R. A. Fjeld, J. T. Coates, D. I. Kaplan, and S. M. Serkiz (2002a). "Plutonium Oxidation State Geochemistry in the SRS Subsurface Environment," Rep. No. WSRC-TR-2003-00035, Rev. 0. Westinghouse Savannah River Company, Aiken, SC.
- Powell, B. A., R. A. Fjeld, J. T. Coates, D. I. Kaplan, and S. M. Serkiz (2002b). "Plutonium Oxidation State Geochemistry in the SRS Subsurface Environment." Westinghouse Savannah River Company, Aiken, SC.
- Powell, B. A., R. A. Fjeld, J. T. Coates, D. I. Kaplan, and S. M. Serkiz. 2002. Plutonium Oxidation State Geochemistry in the SRS Subsurface Environment: Westinghouse Savannah River Company, Aiken, SC. WSRC-TR-2003-00035, Rev. 0.
- Prikryl, J. D., and D. A. Pickett. 2007. Recommended Site-Specific Sorption Coefficients for Reviewing Non-High-Level Waste Determining at the Savannah River Site and Idaho National Laboratory. U.S. Nuclear Regulatory Commission. NRC-02-07-006. Washington, DC.
- Prout, W.E. 1958. Adsorption of Radioactive Wastes by Savannah River Plant Soil. Soil Science. 84:13-17.
- SRNL notebook, "Grout Variability Study" WSRC-NB-2005-00039
- SRNL notebook, "Grout Variability Study II" WSRC-NB-2005-00129
- SRNL notebook, "Grout Variability Study # 3" WSRC-NB-2006-00025
- SRNL notebook, "Grout Variability Study # 4" WSRC-NB-2006-00140
- SRNL notebook, "Grout Variability Study # 5" WSRC-NB-2007-00120
- SRNL notebook, "Grout Variability Study # 6" WSRC-NB-2008-00054
- SRNL notebook, "Grout Variability Study # 7" WSRC-NB-2008-00114

## **7.0 APPENDIX A: SUPPORTING STATISTICAL ANALYSES**

## 7.1 SALTSTONE $K_d$ VALUES

**Table 24. Saltstone Cs, Sr, and iodine  $K_d$  average and standard deviation.**

Sample ID	Cs average	Cs Stdev	Sr average	Sr stdev	I average	I stdev
GVS-93	15.0	3.8	355.0	12.5	3.0	1.9
GVS-94	22.0	2.9	472.0	58.8	0.9	1.1
GVS-100-01	21.0	1.2	809.0	178.1	1.5	0.5
GVS-100-02	208.0	73.3	1685.0	145.6	1.7	1.5
GVS-107	75.0	9.5	592.0	36.7	0.3	1.7
GVS-110	18.0	2.9	530.0	71.8	2.2	0.3
GVS-111	19.0	0.6	718.0	13.3	2.5	1.5
GVS-114	14.0	1.0	414.0	45.1	2.9	0.1
GVS-118	14.0	4.4	385.0	170.6	0.7	0.7
GVS-121	33.0	0.6	1036.0	266.2	1.4	1.8
GVS-123	23.0	5.5	798.0	223.0	0.7	1.6
TR-419	13.0	1.2	544.0	110.1	-0.1	0.8
TR-503	16.0	4.0	323.0	13.3	0.7	0.2
TR-513	22.0	1.5	397.0	88.5	-0.1	0.7
TR-517	14.0	3.0	277.0	16.6	2.1	1.7
TR-531	14.0	4.2	131.0	8.1	-0.1	0.6
TR-614	8.0	1.2	216.0	13.0	0.3	0.6
TR-616	36.0	9.1	943.0	108.6	1.1	0.7
TP-006-003	6.0	1.5	483.0	7.5	-0.2	0.7
TP-006-004	9.0	0.0	398.0	9.2	-0.1	1.2
TP-006-005	8.0	2.5	692.0	30.2	1.3	2.8

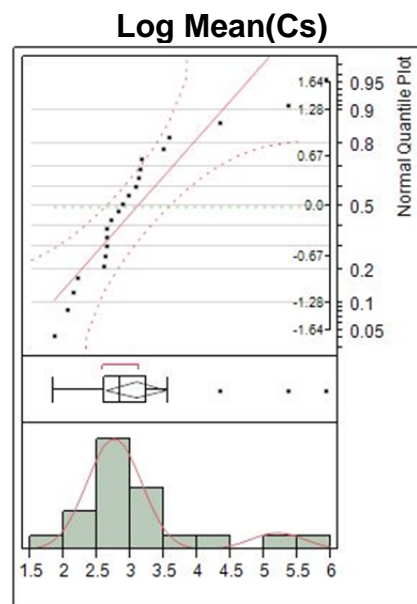
Individual data points presented in

**Table 4 .  $K_d$  values (mL/g) calculated from adsorption experiments for cesium, strontium, and iodine.**

**Table 25. Correlation coefficients for cesium, strontium and iodine saltstone  $K_d$  values and saltstone properties.**

	$Cs K_d$	$Sr K_d$	$I K_d$
$Cs K_d$	1.00		
$Sr K_d$	<b>0.95*</b>	1.00	
$I K_d$	-0.07	-0.06	1.00
Water to Premix Ratio	0.16	0.16	0.39
Al. conc.	-0.15	-0.07	0.29
Max Controlled Cure Temp (°C)	<b>0.60*</b>	<b>0.57*</b>	-0.08
Sample Age (Years)	0.19	0.10	0.17
50% NaOH	-0.01	0.05	0.35
NaNO <sub>3</sub>	0.03	0.06	-0.20
NaNO <sub>2</sub>	0.19	0.27	0.29
Na <sub>2</sub> CO <sub>3</sub>	-0.40	-0.38	-0.05
Na <sub>2</sub> SO <sub>4</sub>	-0.17	-0.10	0.18
Al-Nitrate	-0.29	-0.26	0.16
Na-Phosphate	-0.26	-0.23	-0.09

\* Significant correlation at probability of obtaining a value as large or larger than 0.05 at 21 degrees of freedom,  $r = 0.42$ .

**Figure 7. Histogram of Cs log $K_d$  distribution data of 2-component normal fit demonstrating the potential presence of a second high temperature population.**

Notice the red curve 2-component normal fit to the logged mean data: it overlays the histogram (above).

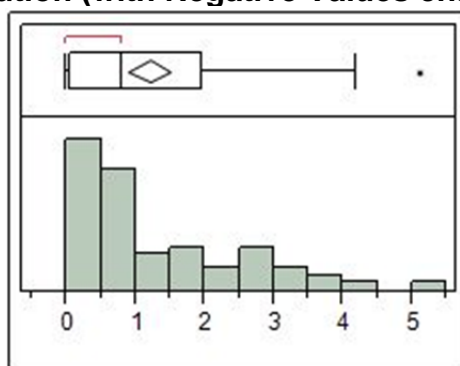
**Table 26. Cs  $K_d$  values (mL/g) as a function of temperature curing ranges**

<b>temperature</b>	<b>n</b>	<b>Cs <math>K_d</math> Median</b>	<b>Cs <math>K_d</math> Mean</b>	<b>Cs <math>K_d</math> Standard Deviation</b>
all	22	17	45	84
60	2	289	289	115
>22	7	14	93	127
<60	20	16	20	15
22	15	18	22	15

These temperature-categories are not mutually exclusive and a  $K_d$  value may exist in more than one category.



# Iodine Distribution (with Negative Values changed to zeros)



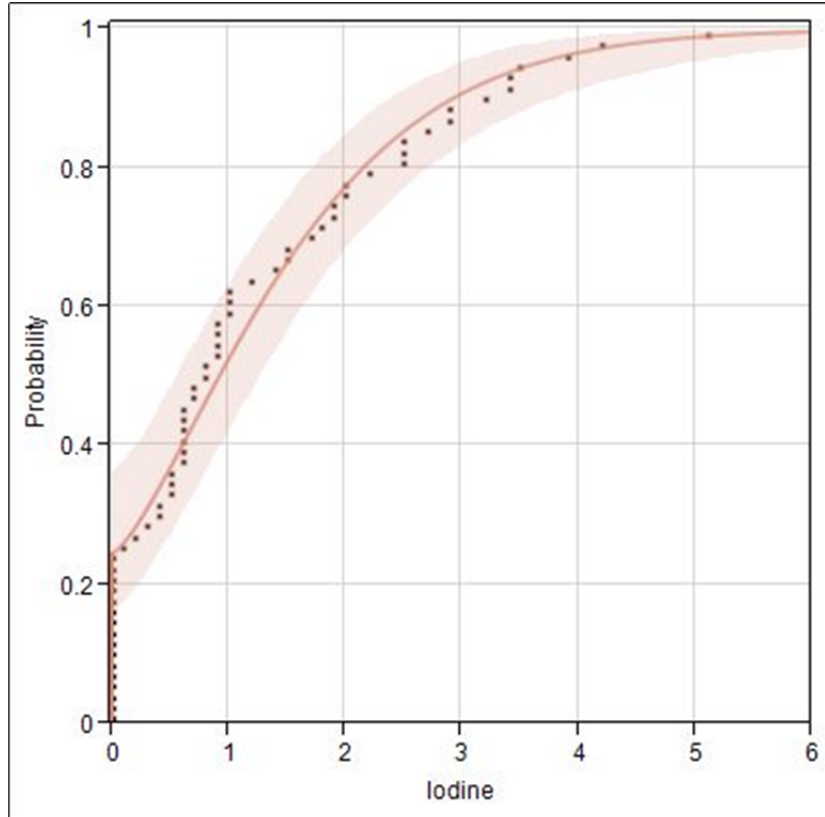
## Quantiles

100.0%	maximum	5.1
99.5%		5.1
97.5%		4.515
90.0%		3.28
75.0%	quartile	1.95
50.0%	median	0.8
25.0%	quartile	0.05
10.0%		0
2.5%		0
0.5%		0
0.0%	minimum	0

## Moments

Mean	1.1984615
Std Dev	1.2495615
Std Err Mean	0.154989
Upper 95% Mean	1.5080877
Lower 95% Mean	0.8888354
N	65
Variance	1.5614038
Skewness	1.1259051
Kurtosis	0.5765588
CV	104.26379

**Iodine Distribution (with Negative Values changed to zeros)**  
**Plot of the Zero-inflated Weibull fit to All of the Modified Iodine Values**



### Statistics

#### Model Comparisons

Distribution	AICc	-2Loglikelihood	BIC
Zero Inflated Weibull	145.93402	139.54057	152.06374
Zero Inflated Lognormal	147.09249	140.69905	153.22221
Zero Inflated Loglogistic	148.90275	142.50931	155.03247
Zero Inflated Frechet	160.82707	154.43363	166.95679

#### Parametric Estimate - Zero Inflated Weibull

Parameter	Estimate	Std Error	Lower 95%	Upper 95%	Criterion	
location	0.5574771	0.10965117	0.3425647	0.7723894	-2*LogLikelihood	139.54057
scale	0.7261876	0.08069536	0.5680276	0.8843476	AICc	145.93402
zero inflation	0.2461538	0.05343035	0.1566221	0.3647321	BIC	152.06374
Weibull $\alpha$	1.7462612	0.19147959	1.4085555	2.1649330		
Weibull $\beta$	1.3770547	0.15302096	1.1307771	1.7604779		

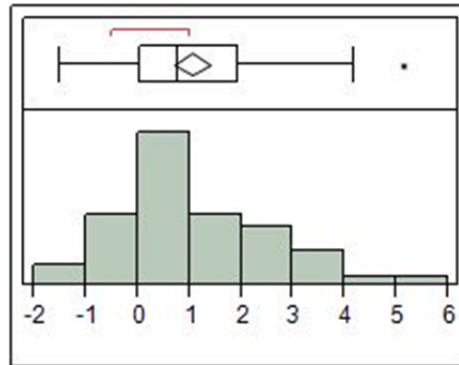
Use a binary variable with probability = 0.24615 that the  $K_d$  is zero and probability = 0.75385 that the  $K_d$  comes from the Weibull distribution below.

#### GoldSim Parametric Estimate – Zero-Inflated Weibull

Parameter	Estimate				
minimum	0.0000				
Slope or shape	1.3770547				
Mean - minimum	1.595841				

Another interesting look at the Iodine data can be gotten if the negatives are left in the dataset.

### Iodine Distribution (Including negative values)



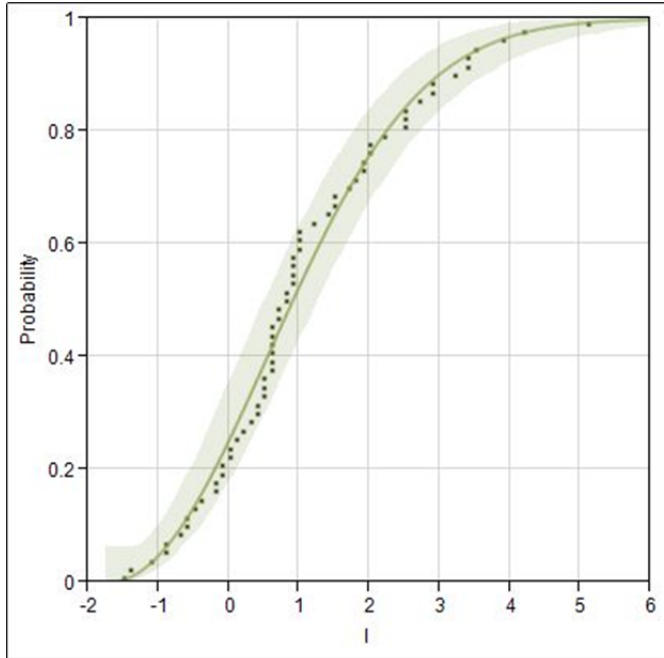
#### Quantiles

100.0%	maximum	5.1
99.5%		5.1
97.5%		4.515
90.0%		3.28
75.0%	quartile	1.95
50.0%	median	0.8
25.0%	quartile	0.05
10.0%		-0.64
2.5%		-1.435
0.5%		-1.5
0.0%	minimum	-1.5

#### Moments

Mean	1.0569231
Std Dev	1.4221429
Std Err Mean	0.1763951
Upper 95% Mean	1.4093128
Lower 95% Mean	0.7045333
N	65
Variance	2.0224904
Skewness	0.6186775
Kurtosis	0.1024054
CV	134.555

### Iodine Distribution (Including negative values) Threshold Weibull fit to All of the Unmodified Iodine Values



Notice that the green line has a y-intercept of about 0.25. This was about the proportion of zeros in the zero-inflated Weibull that you just looked at. As an alternative to the zero-inflated Weibull, you could just use the threshold Weibull with the parameters at the bottom of this page. Whenever you generate a negative value, you just change it to zero.

### Statistics

#### Model Comparisons of zero-inflated Weibull fit of Iodine-Saltstone $K_d$ dataset

Distribution	AICc	-2Loglikelihood	BIC
Threshold Weibull	229.90025	223.50681	236.02997
Threshold Lognormal	230.49271	224.09926	236.62243
Threshold Frechet	231.31360	224.92015	237.44332
Threshold Loglogistic	232.13294	225.73950	238.26266

#### Parametric Estimate - zero-inflated Weibull fit of Iodine-Saltstone $K_d$ dataset

Parameter	Estimate	Std Error	Lower 95%	Upper 95%	Criterion	
location	1.151028	0.11553985	0.924574	1.377482	-2*LogLikelihood	223.50681
scale	0.481412	0.07364688	0.337067	0.625758	AICc	229.90025
threshold	-1.745199	0.25921038	-2.253242	-1.237156	BIC	236.02997
Weibull $\alpha$	3.161441	0.36527241	2.520794	3.964905		
Weibull $\beta$	2.077221	0.31777502	1.598063	2.966768		

#### GoldSim Parametric Estimate – zero-inflated Weibull fit of Iodine-Saltstone $K_d$ dataset

Parameter	Estimate
minimum	-1.745199
Slope or shape	2.077221
Mean - minimum	2.800309

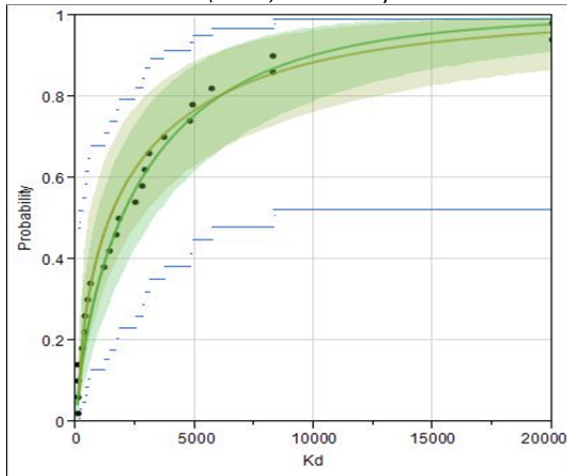
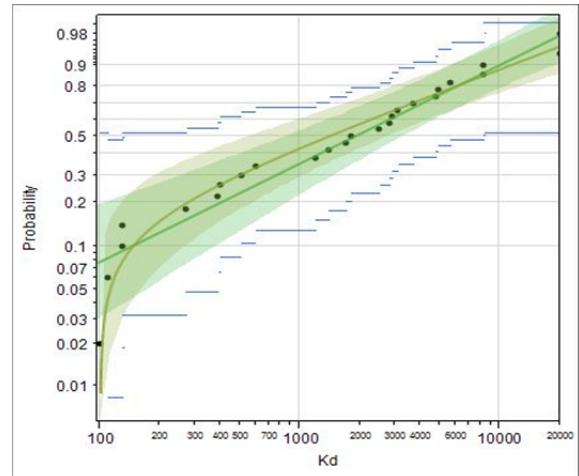
## 7.2 SOIL PLUTONIUM $K_d$ VALUES

**Table 27.** Statistics for relative goodness of fit model comparisons for sand with  $\text{pH} \leq 7$ .

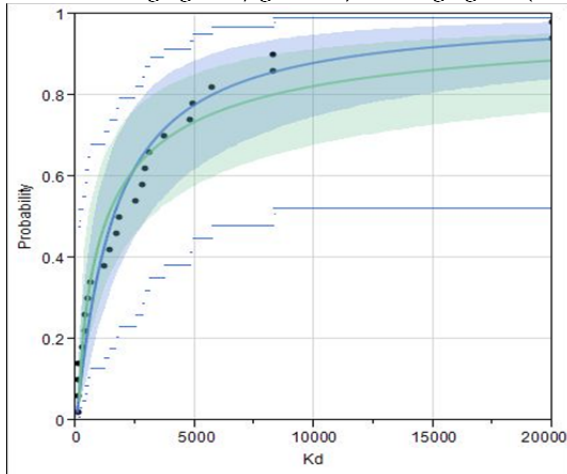
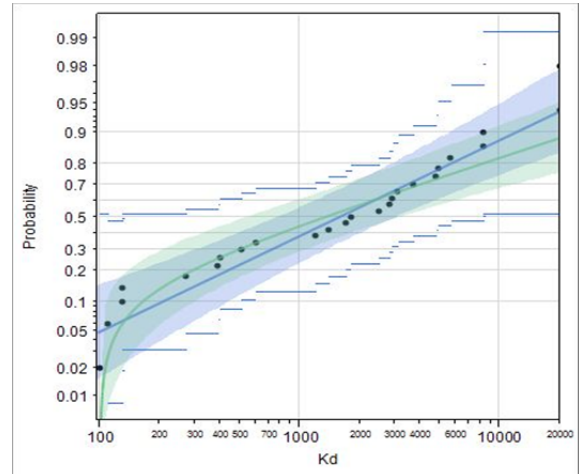
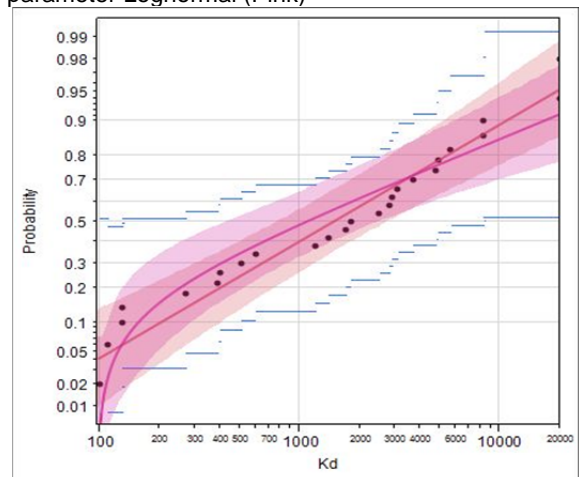
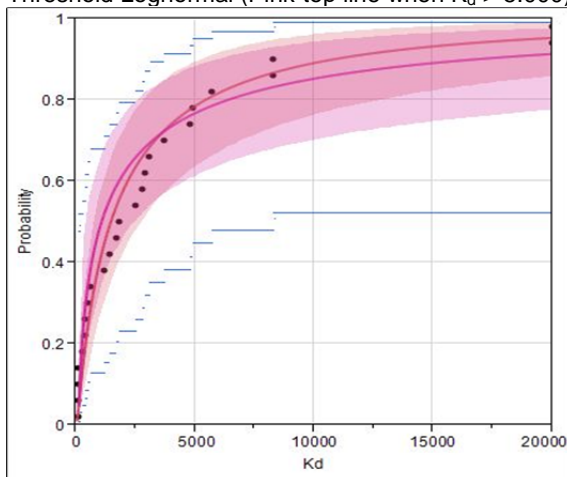
### Statistics for Relative Goodness of Fit Model Comparisons

Distribution	AICc	-2Loglikelihood	BIC
Threshold Weibull	438.18094	431.03809	440.69471
Threshold Loglogistic	449.67123	442.52837	452.18500
Threshold Lognormal	461.41798	454.27513	463.93175
Lognormal	461.69094	457.14548	463.58324
Weibull	462.04200	457.49654	463.93429
Loglogistic	463.47539	458.92993	465.36768
Generalized Gamma	463.90990	456.76704	466.42367
DS Lognormal	464.28834	457.14548	466.80211
DS Weibull	464.63940	457.49654	467.15317
Exponential	464.69969	462.52578	465.74466
Frechet	465.18146	460.63601	467.07376
DS Loglogistic	466.07279	458.92993	468.58656
Threshold Frechet	467.77817	460.63531	470.29194
DS Frechet	467.77886	460.63601	470.29263
Log Generalized Gamma	469.39277	462.24992	471.90654
LEV	486.18709	481.64163	488.07938
Logistic	497.31198	492.76652	499.20427
Normal	504.43632	499.89086	506.32862
SEV	520.96439	516.41894	522.85669

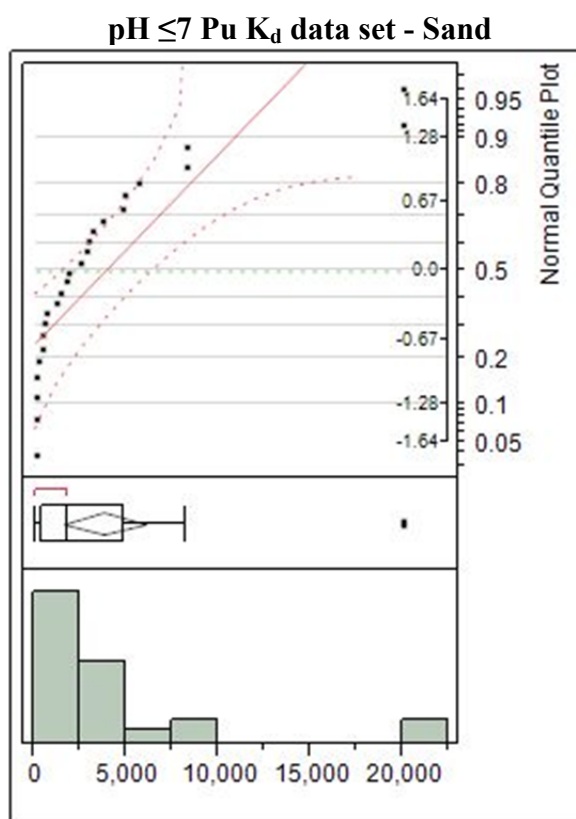
Threshold Weibull (Olive) and Two-parameter Weibull (Green)

Probability vs.  $K_d$  on a linear scaleProbability vs.  $K_d$  (Weibull plots as a line)

Threshold Loglogistic (light blue) and Loglogistic (blue)

Probability vs.  $K_d$  on a linear scaleProbability vs.  $K_d$  (Loglogistic plots as a line)Threshold Lognormal (Pink-top line when  $K_d > 5,000$ ) and Two-parameter Lognormal (Pink)

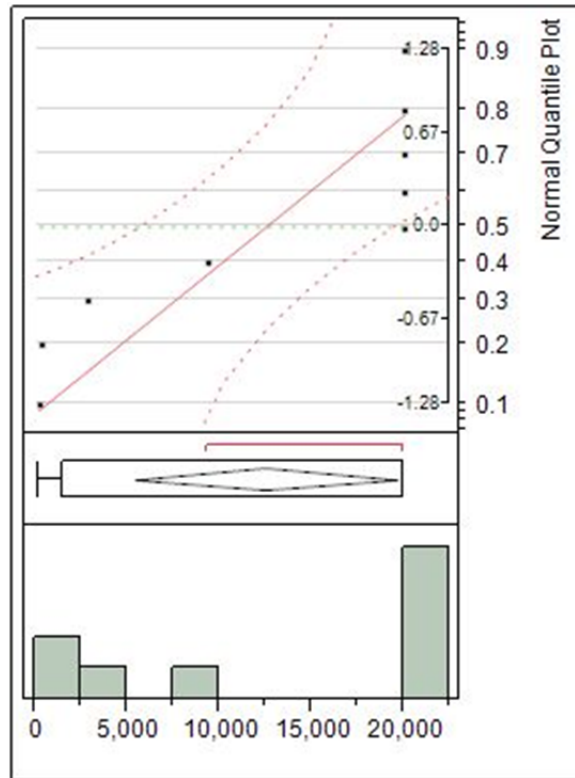
**Figure 8** Weibull, Loglogistic, and Lognormal fits to the sand data for  $\text{pH} \leq 7$ . The left graphs plot the cumulative probability vs.  $K_d$  on a linear scale, and the graphs on the right plot  $K_d$  on a scale that should result in a straight line if the intended distribution is correct.

**Table 28.** Quantile and characterization statistics of the Sand or Clay Pu  $K_d$  values for varying pH ranges.**Quantiles**

100.0%	maximum	20,000
99.5%		20,000
97.5%		20,000
90.0%		12,980
75.0%	quartile	4,850
50.0%	median	1,800
25.0%	quartile	395
10.0%		122
2.5%		100
0.5%		100
0.0%	minimum	100

**Moments**

Mean	3,829.6
Std Dev	5,427.803
Std Err Mean	1085.5606
Upper 95% Mean	6,070.087
Lower 95% Mean	1,589.113
N	25

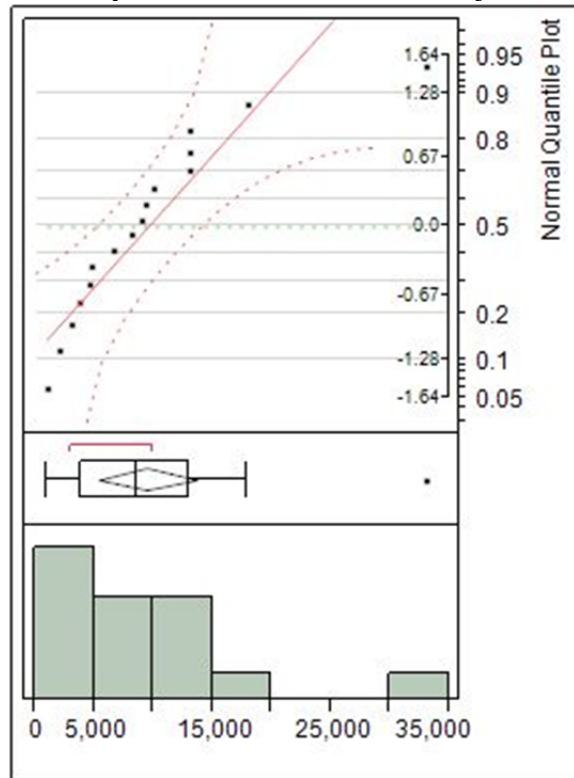
**pH >7 Pu K<sub>d</sub> Data Set - Sand****Quantiles**

100.0%	maximum	20,000
99.5%		20,000
97.5%		20,000
90.0%		20,000
75.0%	quartile	20,000
50.0%	median	20,000
25.0%	quartile	1,545
10.0%		210
2.5%		210
0.5%		210
0.0%	minimum	210

**Moments**

Mean	12511.111
Std Dev	9258.1524
Std Err Mean	3086.0508
Upper 95% Mean	19627.557
Lower 95% Mean	5394.6652
N	9



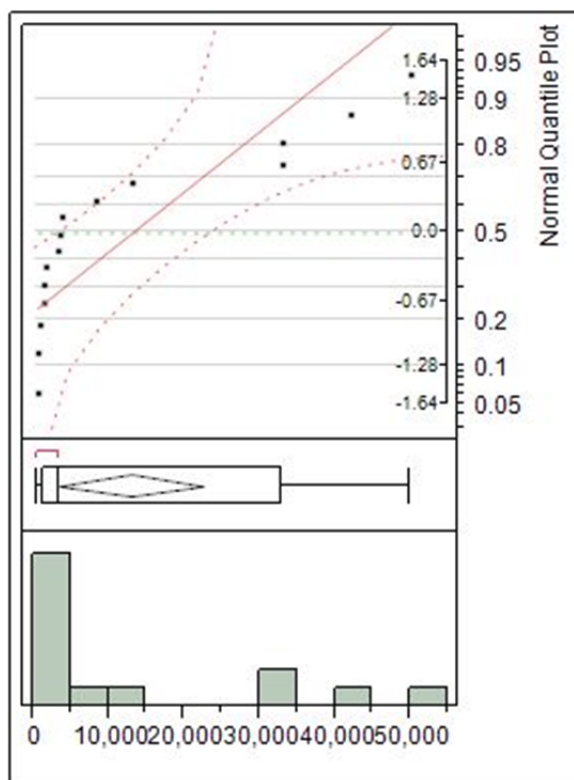
pH  $\leq 7$  Pu  $K_d$  data set - Clay

### Quantiles

100.0%	maximum	33,000
99.5%		33,000
97.5%		33,000
90.0%		22,500
75.0%	quartile	13,000
50.0%	median	8,600
25.0%	quartile	3,925
10.0%		1,770
2.5%		1,000
0.5%		1,000
0.0%	minimum	1,000

### Moments

Mean	9,512.5
Std Dev	7839.3771
Std Err Mean	1959.8443
Upper 95% Mean	13689.809
Lower 95% Mean	5335.1908
N	16

**pH >7 Pu  $K_d$  data set - Clay****Quantiles**

100.0%	maximum	50,000
99.5%		50,000
97.5%		50,000
90.0%		45,200
75.0%	quartile	33,000
50.0%	median	3,500
25.0%	quartile	1,300
10.0%		576
2.5%		540
0.5%		540
0.0%	minimum	540

**Moments**

Mean	13,056
Std Dev	17249.047
Std Err Mean	4453.6847
Upper 95% Mean	22608.204
Lower 95% Mean	3503.7963
N	15

**8.0 APPENDIX B: Pu(IV) AND Pu(V) SORPTION EDGE AT 24 HR OR  
33 DAYS (POWELL ET AL. 2002)**

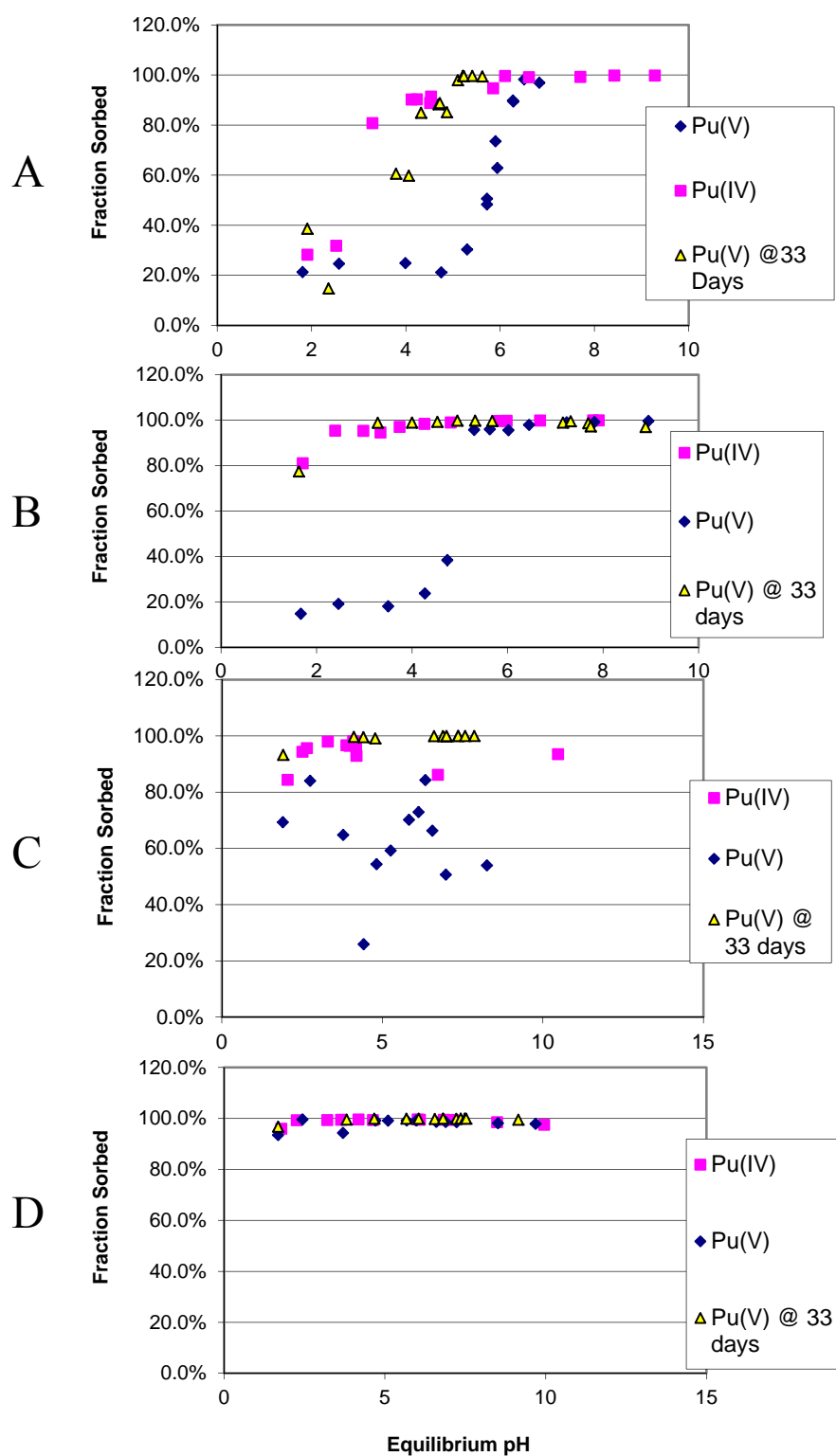


**Figure 9.** Pu(IV) and Pu(V) sorption edge at 24 hr or 33 days on: (A) subsurface sandy sediment, (B) subsurface clayey sediment, (C) surface sandy sediment, and (D) surface clayey sediment (Powell et al. 2002).

## Distribution:

P. M. Almond, 773-43A – Rm. 227  
A. B. Barnes, 999-W – Rm.336  
H. H. Burns, 773-41A – Rm.214  
B. T. Butcher, 773-43A – Rm.212  
L. B. Collard, 773-43A – Rm.207  
A. D. Cozzi, 999-W – Rm.337  
D. A. Crowley, 773-43A – Rm.216  
S. D. Fink, 773-A – Rm.112  
G. P. Flach, 773-42A – Rm.211  
B. J. Giddings, 786-5A – Rm.2  
J. C. Griffin, 773-A – Rm. A-202  
C. C. Herman, 999-W – Rm. 344  
R. A. Hiergesell, 773-43A – Rm.218  
G. K. Humphries, 705-3C – Rm.206  
P. R. Jackson, 703-46A – Rm. 223  
D. I. Kaplan, 773-43A – Rm.215  
C. A. Langton, 777-42A – Rm.219  
D. Li, 999-W – Rm.336  
S. L. Marra, 773-A – Rm. A-230  
F. M. Pennebaker, 773-42A – Rm.146  
M. A. Phifer, 773-42A – Rm.252  
S. H. Reboul, 773-A \_Rm. B-132  
M. M. Reigel, 999-W – Rm.404  
K. A. Roberts, 773-43A – Rm.225  
K. H. Rosenberger, 705-1C – Rm.33b  
E. P. Shine, 702-41A – Rm. 233  
F. G. Smith, III 773-42A – Rm.178  
K. H. Subramanian, 766-H – Rm.2204

(1 file copy & 1 electronic copy), 773-43A – Rm.213